# COOLING RATES OF DUMMIES UNDER VARIOUS DEGREES OF AIR HUMIDITY, WIND SPEED AND AIR TEMPERATURE

A Study Project presented to the Division of Forensic Medicine and Toxicology of the University of Cape Town

In partial fulfilment
Of the requirements for the Master of Medicine in
Pathology (Forensics)

By

Dr Sipho Mfolozi
Student number: **MGDSIP003**
**Division of Forensic Medicine**

**FACULTY OF HEALTH SCIENCES**




Supervisor : **Prof L. J. Martin**

Degree of Confidentiality : **Semi-Confidential**

## DECLARATION

I, Sipho Mfolozi, hereby declare that the work on which this dissertation/thesis is based is my original work (except where acknowledgements indicate otherwise) and that neither the whole work nor part of it has been, is being, or is to be submitted for another digree in this or any other university.

I empower the Univertisty to reproduce for the purpose of research either the whole or any portion of the conents in any manner whatsoever.



Signature:……

Date:……

# TABLE OF CONTENTS

## Special Characters and Mathematical Nomenclature

| | |
|---|---|
| $T_a$ | Temperature of the ambient air, $°C$ |
| $T_c$ | Core temperature, $°C$ |
| $T_s$ | Surface or skin temperature, $°C$ |
| $T_{rectum}$ | Rectal temperature at time $t$ as applied in the Nomogram method, $°C$ |
| $\lambda$ | Thermal conductivity, $W\ m^{-1}K^{-1}$ |
| $\overrightarrow{q_r}$ | Heat flux in the radial direction $r$ |
| $t_0$ | Time of heat withdrawal or time of death |
| $R_\theta$ | Thermal resistance, $(m^2K)/W$ |
| $h$ | Convective heat transfer coefficient, $W\ m^{-2}K^{-2}$ |
| $\alpha$ | Thermal diffusivity $(\lambda\rho^{-1}c^{-1}), m^2s^{-1}$ |
| $\theta$ | Standardised or dimensionless temperature $(T_{rectum} or\ T_r - T_i\ /\ T_\infty - T_i)$ |
| $\rho$ | Density, $kg\ m^{-3}$ |
| $r$ | Any radial distance between the surface and the core (temperature-depth) |
| $r_0$ | Radius of the body |
| $T_\infty$ | Uniform temperature reached by the body at the end of cooling |
| $A/M$ | Surface area/body mass, $cm^3kg^{-1}$ |
| $M$ | Body mass, $kg$ |
| $A$ | Nomogram cooling constant representing post-mortem temperature plateau = 1.25 |
| $B$ | Body-weight dependent Nomogram cooling constant $(kg^{-0.625})$ |
| $T_r$ | Temperature at any radial distance $r$, $°C$. |
| $t$ | Time, $s$ |
| $c_p$ | Thermal heat capacitance, $Jg^{-1}K^{-1}$ |
| $B_i$ | Biot number $(hr_0/\lambda)$, a dimensionless heat transfer coefficient $\lambda_n$ |
| $J_0$ | Zeroth-order Bessel function |
| $J_1$ | First-order Bessel function |
| $clo$ | Unit of thermal resistance by clothing (0.155 K·m$^2$/W) |
| $F_o$ | Fourier number $\tau\ (\alpha\Delta t\ \Delta r^{-2})$ |
| $Re$ | Reynolds dimensionless number (vL/$v$) |
| $Nu$ | Nusselt dimensionless number $(h_sL/k)$ |
| $Pr$ | Prandtl dimensionless number $(v/\alpha)$ |
| $Gr$ | Grashof dimensionless number $[L^3\beta g(T_s - T_a)/v^2]$ |
| v | Velocity, $ms^{-1}$. |
| $\mu$ | Specific viscosity |
| $v$ | Kinematic viscosity $m^2s^{-1}$ |
| $L$ | Travelled length of air over the cooling surface, $m$ |
| $dT$ | Difference of temperature between times $t$ and $t_0$ |
| $f$ | Nomogram corrective factor for cooling conditions different from standard |
| $dt$ | Interval between times $t$ and $t_0 = t$ |

## Abbreviations & Words Unique to this Dissertation

| | |
|---|---|
| TGM | Thermostatic gel manikin |
| CSTG | Core-surface temeprature gradient (arithmatic difference) |
| PMTP | Post-mortem temeprature plateau |
| NTC | Negative temperature coefficient |
| RH | Percentage relative humidity of air |
| PMI | Post-mortem interval |
| PCO untit | Plant Controller |
| LAN | Local area network |
| IP | Internet protocol |
| IT | Information technology |
| Thanatochronometry | •/*noun*/ the science of calculation or mathematical estimation of the post-mortem interval. |

# CHAPTER ONE

## 1.1 **Definition of The Research Problem**

Henssge [1] observed that even a slight but permanent air movement accelerates cooling of a naked body significantly. However in those experimental studies the rate of air movement was not quantified. Today Henssge's Nomogram method of thermometric thanatochronometry (mathematic estimation of the post-mortem interval using body temperature measurements) is used the world over and utilises various corrective factors for naked and clothed bodies in still/moving air. The purpose of this research was to correlate measured air flow rates (wind speed) and measured relative air humidity levels (RH) with post-mortem cooling rate in order to formulate appropriate corrective factors to be used with Henssge's Nomogram. The effect of air flow rates and air humidity on the post-mortem cooling curve was studied within a range of air temperatures using gel-based models (Cooling Dummies) as substitutes for human bodies.

## 1.2 **Background and Literature Review**

Accurate estimation of the interval of death has obvious importance to the legal and justice system of any nation, especially in cases in which the cause of death is suspected to be criminal in nature. From before antiquity it had been known that bodies cool after death, and as forensic medicine became recognised as an independent discipline, a large proportion of research in this field focused on understanding post-mortem cooling in order to describe accurate methods of thanatochronometry. The first known record of measured post-mortem body temperature was undertaken by Dr John Davey [2], who did not attempt to derive a formula or method of thanatochronometry but could appreciated the significance of post-mortem thermometry in medical jurisprudence.

The first author to take serial post-mortem temperature measurements from a body was Dr Benjamin Hensley [3] of Philadelphia in 1846 who only recorded the measurements and also did not attempt to describe a mathematical formula or method of thanatochronometry. In 1863 Taylor and Wilkes [4] carried out temperature measurements from 100 bodies and described for the first time the existence of the post-mortem temperature plateau (PMTP). They also discussed the influence of clothing, environmental temperature, a heat gradient and insulation of the deep core of a body. They cautioned on use of judging skin temperature using the hand and advised use of internal body temperature. In 1868 Rainy [5] was the

first author to uniformly use rectal temperature measurements and was also the first author to introduce mathematical concepts into the field. For the first time he mentioned Newton's Law of Cooling [6] which states that "the rate of change of the temperature of an object is proportional to the difference between its own temperature and the ambient temperature". Rainy stated that Newton's Law was not absolutely correct when applied to post-mortem cooling. He also noted the presence of a PMTP in 46 bodies from which he had measured rectal temperature. He offered a mathematical formula for estimating the PMI that required the use of algorithms, which he conceded underestimated the PMI due to the effect of the PMTP.

The first time a temperature graph was used to illustrate post-mortem cooling was in 1880 by Burman [7] who showed a rate of temperature fall over unit time. His temperature graphs from axillary measurements did not show the PMTP, but in fact showed that the temperature drop was most rapid soon after death, presumably because axillary temperature closely correlated to that of skin than to core temperature. Following on the work of Taylor and Wilkes, Womack [8] used complex mathematics, including calculus, which involved Newton's Law of cooling as well as the use of body mass and surface area. He was also the first to use temperature units converted from Fahrenheit to centigrade. He also acknowledged the effect of body covering on his thanatochronometry method.

In 1953 Schwarz and Heidenwolf [9] suggested that rectal temperature measurement should be added into other methods of thanatochronometry as part of the routine examination of a body by police surgeons. They discussed physical aspects of post-mortem cooling and observed cooling rates from different parts of the body. Presence of the PMTP was also noted form rectal temperature curves, but noted its absence from skin temperature curves. They also noted that the skin temperature dropped precipitously immediately after death and during which a large temperature gradient between the core and the skin developed. They did not offer a formula for thanatochronometry.

In 1954 Shapiro [10] commented on the claimed accuracy of many thermometric thanatochronometry methods and their medico-legal impact. In 1965 Shapiro [11] was the first author to make use of the term 'post-mortem temperature plateau' to refer to the slow initial rate of core cooling, which today is standard practice. Two years before, Shapiro had noted the PMTP on a body that had been dead for at least four hours. His explanation of the PMTP was that it was that cooling at the centre of the body is delayed until a temperature gradient is established by conduction from the centre to the periphery.

In 1955 de Saram [12] attempted to quantify, through a mathematical formula, heat loss from the body by thermal radiation, thermal convection and by thermal

conduction by measuring the effects of ambient temperature, air humidity, surface area, evaporation et cetera on the rate of post-mortem cooling of 41 executed prisoners. Using rectal temperature measurements taken at a depth of 3 to 4 inches (7.62cm to 10.16cm) he also described the presence of the PMTP immediately after death which he described as being caused by a delay in the establishment of a temperature gradient from the core as well as well as by post-mortem metabolism. To allow for the PMTP he added an arbitrary 45 minutes into his calculated time of death. de Saram was the first author to suggest that the body surface area to body mass ratio $A/M$ affected the rate of body cooling. The simplified mathematical formula he derived had two constants.

In 1956 Lyle and Cleveland [13] used continuous multi-channel temperature recordings from six body sites, including the skin and brain, and used a differential temperature between the body and its surroundings. There was no PMTP in their study, presumably because of long PMI before thermometry. They did not describe a practical method of thanatochronometry. In 1957 de Saram and Webster [14] advised that any thanatochronometry formula must use corrective factors for the variable circumstances of cooling rather than the use of a simple from which the result is then adjusted.

In 1959 Fiddes and Patten [15] introduced a percentage method in which they constructed an exponential curve that became linear when plotted on an algorithmic graph. Their observed cooling rate of 1.5°F over the first 12 hours had a wide range of variation of up to 70% variation on either side. They stated that external factors such as body covering and ambient temperature had little effect to this method and, for the first time, used the model of a cylinder of infinite length to explain post-mortem cooling. Fiddes and Patten did not accept the approach of empirical adjustment of the PMTP used by de Saram, but attempted to determine it for each individual calculation.

In 1958 Sellier [16] explored the theoretical aspects of post-mortem cooling which he noted to be similar to that of a cylinder of infinite length. He pointed out that the body radius has much more of an influence on the shape of post-mortem cooling curve than do cooling conditions and suggested that the PMTP, whose presence he observed in his own studies, could be explained purely by elemental physical considerations, specifically the existence of a temperature gradient, which he also attributed to the delay in the establishment of a temperature gradient to the core. He mentioned that core-cooling occurs only when a 'cooling wave' reaches the core, whose amplitude has no effect on the propagation rate. He noted a very rapid rate of skin cooling immediately after death/heat withdrawal, and noted that after 15 minutes of cooling the temperature decrease only penetrated an outer layer of

2cm thickness. His extrapolation method had a claimed error margin of 30 – 40 minutes under favourable conditions; otherwise it was only 1 hour.

The 1960's were dominated by Marshall whose work on post-mortem cooling and thermometric thanatochronometry began with a thesis [17] in 1960 and was followed by several other papers [18,19, 20, 21, 22, 23, 24]. In 1962 Marshall and Hoare [22] measured core temperatures of recently-deceased human bodies and noted that, unlike the single exponent cooling curve predicted by Newton's Law of cooling, post-mortem cooling curves of the deep rectum (the core) had a double-exponential or sigmoid shape with (i) an initial PMTP of *slow* cooling lasting up to five hours, (ii) a practically straight portion of varying length and slope and (iii) a slow-falling curve similar to that usually associated with cooling expressed by Newton's Law. They also noted that the PMTP, together with the practically straight part of the cooling curve, were the most variable parts of the curve, and concluded that Newton's Law of cooling was not valid in the first 12 hours after death. They observed slight differences in shapes of time-temperature curves plotted from rectal and liver measurements, and large differences in the shapes of core curves (both rectal and liver) in comparison to curves plotted axillary temperature measurements. Marshall and Hoare devised a mathematical formula, known as the Cooling Formula, with two exponential terms that express post-mortem cooling from rectal temperature measurements:

$$\theta = A\,e^{(Bt)} + (1 - A)\,e^{\left(\frac{A \times B}{A-1} \times t\right)} \quad (1)$$

where $A$ = a constant; $B$ = a constant and $t$ = death time. The second exponential term, which has the constant $A$ as an exponent, describes the PMTP. The first exponential term, which has the constant $B$ as an exponent, expresses the exponential drop of the temperature after the post-mortem temperature plateau according to Newton's Law. The first exponent expresses cooling proportional to temperature excess of the body over its environment; the other expresses the influence of modifying factors. The formulation of the Cooling Formula was applauded as the ultimate success in modelling body cooling for the applied purpose of thanatochronometry.

In 1965 James and Knight [25] conducted a survey that compared known PMI intervals with calculated values in 100 bodies using a simple linear calculation with arbitrary modifications that were based on their own experiences. Their survey showed substantial errors in which underestimation of the PMI was more common. They noted an increase of the absolute error in the relationship between actual and calculated PMI. In 1970 Joseph and Shickele [26] published a paper on the physics of body cooling and, as Sellier and Fiddes and Patten had done before them, they used the analogy of a cylinder of infinite length to describe post-mortem cooling. Joseph and Shickele discussed the importance of radius of the cylinder, referring to it as the 'location factor'. Their description of body cooling

was that there is a migration of a temperature gradient. They attributed the PMTP to a small temperature gradient existing at the core. They stated that measuring the temperature of skin or clothes was not necessary, as long as resistance of heat flow from the core through different barriers to the external environment was considered as a single entity whose magnitude can be derived by simple addition of the individual resistances of the different components. They suggested the application of *clo* units to represent surface insulation by clothing. Joseph and Shickele, however, did not offer a practical method of thanatochronometry.

In 1974 Brown and Marshall [27] published a paper on the theoretical basis of the PMTP. They realised that Newton's Law of Cooling fails to account for the PMTP and reasoned that the Law relates to body size and thermal properties that do not apply in the human corpse. In 1977 Simonsen *et al* [28] used continuous temperature measurement from five different sites in the body in uncontrolled cooling conditions and found brain thermometry to be most consistent. They noted that accuracy of thanatochronometry diminished with increasing PMI. In 1979 and 1980 Keuhn [29,30] investigated validity of Newton's Law and found it unsuitable to account for post-mortem cooling in dogs, devising instead a complicated biological model. In 1980 and 1981 Hiraiwa and co-workers [31, 32] used de Saram's rectal temperature measurement data to estimate the PMI using CT scan images of the human torso applied to a computer model based on the cylinder of

infinite length. They also studied the relationship between skin and rectal temperature.

From the late 1970's and early 1980's Henssge [33, 34, 35, 36] extended the work of Marshall's thanatochronometry method of rectal thermometry and became one of the prominent contributors in the field. He introduced concepts such as 'Standard Cooling Conditions' in which a naked body is in the supine position, on a thermally indifferent surface, and cools in constant air temperature with no wind and no strong thermal radiation. The supposed reasoning was to minimise the effect of environmental variables on the rate of body cooling so that experimental conditions can be reproduced and experimental data can be handled safely. The other concept he introduced was that of 'pilot-broken studies' in which one or more external parameter that affected post-mortem cooling rate was changed 'mid-flight'[37, 38]. The presence of the PMTP was observed in many of his studies. Henssge was also the first author to use gel thermal manikin, colloquially referred to as cooling dummies, as substitutes for corpses in cooling studies. Cooling curves from these cooling dummies also showed the PMTP. He empirically determined the value for the cooling constant $A$ of the Cooling Formula to be 1.25 and found a strong correlation between the cooling coefficient $B$ of the Cooling Formula and body mass to the power of – 0.625. In 1988 Henssge [1] developed the Nomogram method based on the Cooling Formula, whose mathematical expression is:

$$\theta = 1.25e^{Zt} - 0.25e^{5Zt} \quad (2)$$

where $Z$ is –1.2815 ($f$ x $M^{-0.625}$) + 0.0284; $f$ is the correction factor for cooling conditions differing from standard conditions; and $M$ is the body mass. Henssge performed several series of cooling experiments under various cooling conditions using naked bodies under permanent moving air, different types of dry clothing and covering, wet clothing and body cooling in still water. He empirically derived corrective factors for those variables whereupon, for example, a clothed body would cool like a naked body that is 1.4 times heavier, and therefore a corrective factor of 1.4 would have to be utilized in the Nomogram method.

The permanently moving air for which Henssge empirically determined corrective factors was produced by a small 25W fan that was mounted on the ceiling at a distance of about 2 meters from the body surface, and it produced 'only a very slight air movement'. The speed of the air movement was not quantified. Higher air flow rates would reasonably be expected to result in expedited surface cooling, which would result in accelerated core cooling than lower air flow rates.

Henssge also collaborated with many other authors, describing corrective factors for bodies covered by leaves [61] and applying the Nomogram method in the field [39]. He also examined dependence of corrective factors on body weight under stronger thermic insulation conditions [40] and described integration of different methods of thanatochronometry, including electromechanical methods [41, 42, 43,

44]. From 1986 Al-Alousi introduced microwave thermography [45, 46, 47, 48, 49, 50, 51], a non-invasive thermometry method of different body parts, and devised the triple-exponential formula (TEF):

$$\theta = P_1 e^{P_2 t} + P_3 e^{P_4 t} + P_5 e^{P_6 t} \quad (3)$$

where $P_1 - P_6$ are parameters or constants: parameters $P_1$, $P_3$ and $P_5$ are referred to as intercept-parameters and parameters $P_2$, $P_4$ and $P_6$ are referred to as exponent-parameters. Al-Alousi found that intercept-parameter did not vary from curve to curve, while exponent parameters varied from case to case. With microwave thermography method the temperature-depth varied anywhere between 1.6cm and 10cm depending on the amount of water content in tissues. The mid-1980's also saw the emergence of internal-body-temperature-only methods of thanatochronometry [52, 53, 54] in which the gradient of the cooling curve is calculated from two core temperature measurements taken at two separate times. These 'self-contained' methods can be traced back to the mathematical reasons given by Marshall and Hoare [22] of the invalidity of Newton's Law for describing post-mortem. They do away with measurements of external factors that affect core-cooling such as ambient air temperature. The time-dependent Z equation on which these methods are based is:

$$\frac{dT}{dt} = -Z\,(T - T_a) \quad (4)$$

where the temperature $T$ is of the body, $T_a$ is the ambient air temperature and $Z$ is the body size factor.

The problematic subject of the PMTP was once more addressed in 1985 by Nokes [55] who suggested that it may be the result of post-mortem heat production from anaerobic glycogenolysis and perhaps even by a small degree of autolysis. In 2002 Nelson [56] reiterated and agreed with this hypothesis. Al-Alousi [49] asserted that for the PMTP to occur there must be little or no cooling. Smart [57] stated that the appearance of the PMTP is a random and unpredictable phenomenon that depends on multiple inter-individual factors such as the body temperature at death, drugs, electrolytes, biomarkers *et cetera*, including post-mortem anaerobic glycogenolysis.

Turn of the 21st century saw the introduction of sophisticated computerised thanatochronometry methods. In 2005 Mall [58, 59] used the Heat-flow Finite Element Model, a numerical procedure for solving partial differential equations under complex geometrical, *initial* and *boundary conditions* of heat transfer that is often applied in engineering design and in many speciality fields that involve heat transfer. Mall's approach to its application was based on Marshal and Hoare's method of rectal thermometry which had been established as the gold-standard route to represent core temperature. He applied it to both 'Sandard Cooling Conditions' and 'pilot-broken studies' in a manner similar to Henssge's approach.

Smart [60] applied a Fourier series unsteady-state heat transfer model – another numerical procedure for solving conditions of complex heat transfer – to unsteady-state heat transfer of a wooden cylinder suspended from a height, whose thermal diffusivity is approximate to that of the human trunk. Smart measured the temperature of the wooden cylinder from a location off its geometric centre, whose axial distance is comparable to the anatomical distance of the human rectum from the centre of the trunk. Time-temperature curves of the wooden cylinder also displayed the PMTP. Like Mall before him, Smart compared his model to Henssge rectal Nomogram method.

# CHAPETER TWO

## 2.1 **Research Hypothesis**

In life air flow (wind) casues the perceived temperature to be lower than the actual air temperature, a phenomenon known as the 'wind chill factor'. The purpose of this research study was to establish corrective factors for measured wind flow rates to be used in the Nomogram method, the ultimate purpose being to make thanatochronometry using this method to be more accurate.

During life it is general knowledge that high air relative humidity results in high discomfort levels, especially in summer months. This is due to ineffectiveness of sweating – the body's mechanism of dissipating heat – due to the fact that already high water content in the surrounding air does not favour evaporation of sweat. In inanimate objects high humidity in the surrounding air also results in rapid cooling compared to low air humidity because of the inherent heat-absorbing property of water carried in the air. Therefore relative air humidity can also be expected to affect the cooling rate of a body after death. The combined effect of high relative humidity, low air temperature and high air flow speed can be expected to have a maximum effect of accelerating post-mortem body cooling than any other combination of the three factors. In this regard the purpose of the research study is to establish corrective factors for measured air relative humidity and air

temperature to be used in thanatochronometry, the ultimate aim being to make death interval estimation more accurate.

Regarding Cooling Dummies, the hypotheses upon which the study was based are that:

1. Relative air humidity is directly proportional to the surface cooling rate of a body. In turn, increased surface cooling rate causes increased core-cooling rate.
2. Air flow speed is directly proportional to the surface cooling rate. In turn, increased surface cooling rate causes increased core-cooling rate.
3. As air temperature is known to be inversely proportional to the cooling rate of the surface, it is hypothesized that surface cooling rate will be significantly high in environments with low air temperatures, high humidity and high wind speed.

## 2.2 Aims and Objectives

*Aims*

The aim of this study was to describe a new set of corrective factors for measured wind flow rates, air relative humidity and air temperature – which would be referred to as ***velocity humidity temperature (VHT)*** factors and used in calculations of the PMI. This study project made use of human body substitutes known as Cooling Dummies, which have similar heat transfer characteristics to human corpses. Various combinations of air speed, humidity and temperature were artificially generated in a controlled environment. The ranges of these parameters were meant to be comparable to indoor and outdoor conditions expected in most parts of the world during all seasons of the year.

*Objectives*

The objectives of this study were:

1. To establish a climate-controlled laboratory in which air temperature, air flow rate (speed) and air relative humidity could be artificially generated and adjusted to specification.
2. To fabricate two pairs of large Cooling Dummies representing adults and two pairs of small Cooling Dummies representing small adults/children.
3. To acquire and use a static incubator for warming Cooling Dummies.

4. To log data of core temperature measurements of Cooling Dummies during cooling experiments that would be carried out in the controlled-climate laboratory.
5. To plot and compare cooling curves of each Cooling Dummy under various combinations of wind speed, air temperature and relative humidity.
6. To derive a set of corrective factors for each combination of the three weather variables to be used during calculations of the post-mortem interval when the same values of the weather variables around a corpse are available.

# CHAPTER THREE

## Research Design and Methodology

### 3.1 The Climate-controlled Laboratory

Cooling experiments were conducted in a special climate-controlled laboratory that was purpose-built for this study project on the second floor of the Division of Forensic Medicine, Falmouth Building, Medical Camps of the University of Cape Town, South Africa. The laboratory consists of two separate rooms, namely the climate-controlled experiment chamber located in room 2.04, and the experiment-monitoring room located in room 2.01. The two rooms are approximately 10 meters apart. Cooling experiments were conducted in the controlled-climate chamber and monitored in the monitoring room.

The climate-controlled laboratory artificially creates a climate in which the air temperature can be varied from –10°C to above +60°C; in which the air relative humidity (RH) can be varied from ~10% to 100%; and in which the wind speed can be varied from 0km/h to above 54km/h. The laboratory was designed to be able to attain and maintain any desired combination of these three factors. The only technically possible way in which the climate-controlled laboratory attains these objectives was through the use of computerised control system in conjunction with industrial hardware.

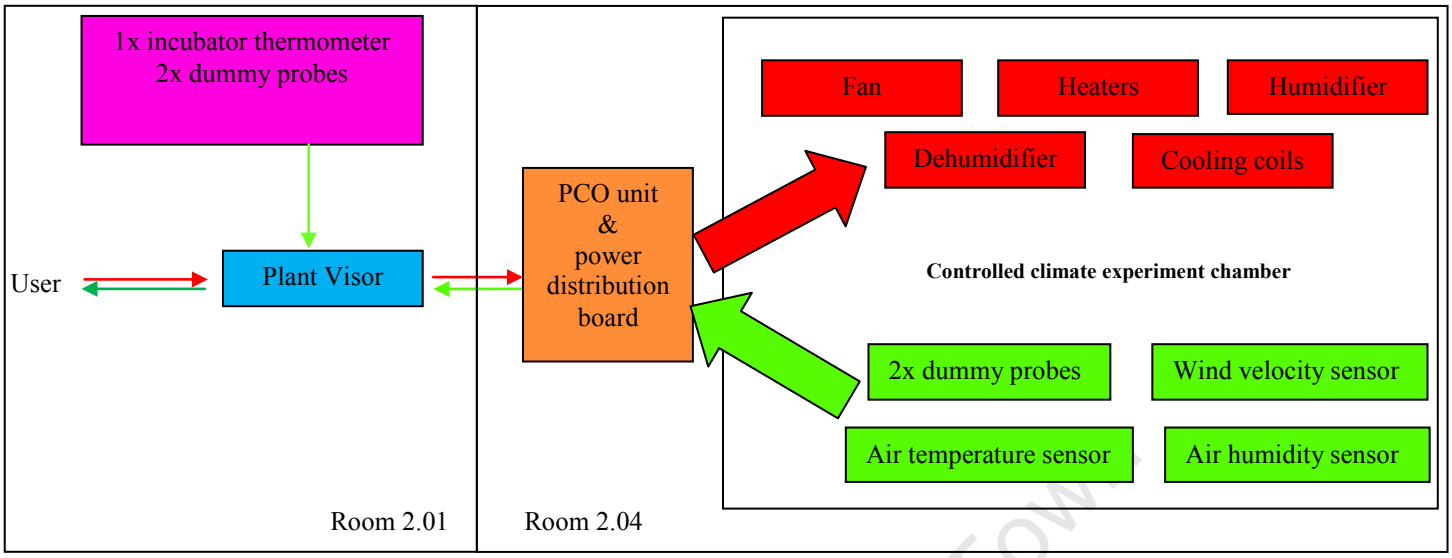


Figure 1 shows a schematic representation of the functionality of the climate-controlled laboratory. Red arrows indicate input commands, green arrows indicate measurements. Red boxes indicate climate-altering equipment, green boxes indicate sensors.

### 3.1.1 The Climate-Controlled Experiment Chamber

The climate-controlled chamber is essentially a cold room that was built inside room 2.04 a number of years ago. The chamber is approximately 3.3 m x 2.2 m x 3.9 m in size. It has an approximately 100mm thick concrete floor that was built onto the floor of room 2.04. Thermal insulation panels form the walls and roof of the cold room. Each thermal insulation panel is made of a ~95mm thick polystyrene sheet sandwiched between 2mm galvanized metal sheets. Access into chamber is through a freezer-type door located on the east wall.

After acquisition of the cold room a false ceiling made from a 45mm thick thermally insulated polystyrene panel was fitted. The false ceiling was suspended from the true ceiling by 440mm long steel rods. It allowed for effective air circulation throughout the chamber. The false ceiling is fixed against the east and west walls of the chamber, terminated one meter from the south wall of the chamber and 0.5 meters from the north wall, and rested on two vertical and parallel 45mm thick thermally insulated panels that rest on the concrete floor. These panels were oriented north-to-south and are equidistant from each other and from the east and west walls of the chamber. They effectively divided the climate chamber into three parallel, communicating and roughly equal compartments under the false ceiling. Light in the climate chamber was provided by a 1600mm long fluorescent light fitting on the roof with two fluorescent light tubes. A Perspex window measuring 1600mm x 300mm was fitted in the middle section of the false ceiling to transmit light. As a result the two side compartments were slightly darker. There was a single 40W tungsten light bulb fitted on the south wall that provided additional light to the climate chamber.

### 3.1.2 The PlantVisorPRO®

The PlantVisorPRO® (Photo 1) is a specialized desktop computer that has a monitor, tower, keyboard and mouse. The PlantVisorPRO® is manufactured by the Italian company Carel and was placed in the experiment monitoring room. The PlantVisorPRO® is a limited-functionality computer that runs Windows XP Embedded Edition® with Internet Explorer 8. It is a web server, so that when connected to an ADSL router with a public IP, it can be accessed via the Internet. It is also a data logger that was programmed with custom software which enables the user to:

1. Enter settings of wind speed, relative air humidity and air temperature to be achieved in the climate chamber.
2. Relay requested settings of wind speed, relative air humidity and air temperature to the PCO Unit (Plant Controller Unit).
3. Monitor and record real-time measurements of air temperature, relative air humidity, and wind speed; of two Cooling Dummy core temperatures from the controlled-climate chamber via from the PCO Unit; of incubator temperature and of two Cooling Dummy core temperatures inside the incubator. The PlantVisorPRO® stores measured data in its internal hard drive.

The PlantVisorPRO® was connected to the University's local area network (LAN) and was assigned with its own static internet protocol (IP) address by the University's IT Department and was granted with firewall exception. Thus the PlantVisorPRO® could thus be remotely accessed by authorised persons from any computer outside the university network in order to change experiment settings or to monitor the status of an experiment. The PlantVisorPRO®'s World Wide Web address is https://137.158.231.101/PlantVisorPRO/.

Photo 1 shows the PlantVisorPRO® in room 2.01 with LED monitor and keyboard

### 3.1.3 The Electric Distribution Board and PCO Unit

The electric distribution board and PCO Unit were functionally positioned between the climate-controlled chamber and the PlantVisorPRO® and were located in room 2.04. Their combined functions were to:

1. Supply electrical power to all the various hardware in the controlled climate experiment chamber. The main distribution board utilise a 30 Amp (400 V / 50Hz) three-phase electric power supply that had to be pulled from an electric substation within Falmouth Building. The electric power to all various equipment in the experiment chamber came directly from this board and was controlled by the PCO unit. This arrangement allowed the PCO unit to regulate switching timing for various pieces of hardware inside the climate chamber.
2. Translate and adjust digital signals from the PlantVisorPRO® into meaningful electrical control output signals to the specific pieces of equipment in the chamber,
3. To synchronise the timing of each hardware piece in order to maximise efficiency,
4. Translate inputs from various sensors in the climate chamber back into electronic signals for the PlantVisorPRO®.

5. To adjust the outputs of the various pieces of equipment according to the signals received from the various sensors using a negative feedback loop,

The main distribution board was an 80kg, wall-mounted metal box 300mm x 1000mm x 800mm in size (Photo 2). Inside it there was the PCO Unit also manufactured by Carel – a small electrical device roughly 225mm x 110mm x 55mm in size (not shown).




Photo 2 shows the main distribution board in room 2.01 that houses the PCO unit

### 3.1.4 Air Cooling System of the Climate-Controlled Laboratory

The air cooling system consisted of a heat exchanger whose purpose was to lower the air temperature in the climate-controlled chamber by removing heat from the air into the external environment. Components of the heat exchanger system were:

1. Cold-room type cooling coils (Photo 3) mounted on the roof of the climate-controlled chamber towards the north wall. The coils had two blower fans, each approximately 250mm in diameter. Blown air travelled within the false ceiling and came into contact with air-heater elements (see later) just before the false ceiling terminated towards the south wall. Power supply to the blower-fans was independent of the PCO unit.
2. A compressor unit (Photo 4.) that was situated on the first floor of the Division of Forensic Medicine. The compressor had a reserve tank of refrigerant gas, a radiator and a fan similar to that of an automobile engine. Warm refrigerant gas returning from the cooling coils in the controlled-climate chamber passed through the compressor unit and lost heat during compression. The cold refrigerant gas was then pumped back into the climate-controlled chamber.
3. An insulated pipe that conveyed the cold refrigerant gas from the compressor back to the cooling coils.

4. A solenoid valve (Photo 5) that controlled flow of refrigerant gas from the cooling coils to the compressor for cooling. The solenoid valve was connected to and controlled by the PCO Unit via the blue wires. When cooling was not required, the PCO Unit shut down refrigerant gas flow via the solenoid valve, while the blower fans continued unhindered to produce air-mixing in the chamber.



Photo 3 shows cold-room type cooling coils with two blower fans is positioned between the white false ceiling and the chamber roof.

Photo 4 shows the compressor unit of the heat exchanger. Note the radiator, fan and tank.

Photo 5 shows the solenoid valve interrupting the un-insulated pipe carrying refrigerant gas to the compressor unit. Note the black insulated pipe below it.

### 3.1.5 Air Heaters

Three U-shaped heating elements encased in an open rectangular metal cage (Photo 6) were placed on the false ceiling just before it terminated towards the south wall. The electric supply to the heaters, as well as commands of when to switch on or off, came from the PCO unit. Each heating element had a power rating of 1KW. The heater was fitted with a pressure differential safety mechanism consisting of two air pressure sensors: one was placed in front and the other placed behind the blower fans. When the blower fans were switched off for whatever reason the safety mechanism activated and turned the heaters off to avoid overheating and risk of fire.



Photo 6 Three heater elements on the false ceiling. Note the cooling coils in the background on the left and the false ceiling suspension rod in the foreground.

### 3.1.6 Air Humidifier

Humidification of the air in the controlled-climate chamber was produced by a Model **UE018 humiSteam x-plus®** electrode boiler manufactured by Carel. The humidifier was 365mm x 275mm x 712mm in size (Photo 7). Because the humidifier has sensitive electronic equipment that could be damaged by high air humidity, it was mounted on the outside of the east wall of the climate-controlled chamber. Water to the humidifier was supplied via a copper pipe from an adjacent room to which a cup-like Perspex filter (Photo 7) was fitted to protect the humidifier of impurities in the water supply. This model humidifier comes with its own built-in PCO Unit, but for purposes of this laboratory that PCO Unit was deactivated and overridden by the PCO Unit in the distribution box from which the humidifier derived its electric power, instructions of how much steam to produce and timings to produce it. The maximum steam production capacity for this humidifier was 18 kg/h.



Steam from the humidifier was conveyed via a blue steam tube that had a 30mm internal diameter. The tube passed through the east wall of the climate chamber (Photo 8). Inside the chamber steam was dispensed by a 560mm long stainless steel tube dispenser fitted at the end of the steam tube. The steel tube dispenser was fixed to the south wall of the chamber. It had seventeen 5mm round apertures (Photo 9) through which steam was pumped. Even though the seventeen apertures

faced the roof of the climate chamber, steam from them was immediately drawn downwards by air flow from the blow-fans of the coils (and by the fan, mentioned next).

Photo shows the Carel humidifier outside the east wall. Note the blue steam pipe going through the wall from the top. A brown copper water pipe with a water filter is beneath the humidifier.

Photo 8 shows the steam delivering pipe inside the chamber.


Photo 9 shows the steel tube steam dispenser. Note the 17 apertures through which steam is dispensed.

### 3.1.7 Air Dehumidifier

Air dehumidification was achieved to a lesser extent by the heat exchanger mentioned previously. When dehumidification was required, the PCO Unit opened the solenoid valve and cooling began. At the same time the PCO Unit switched the three heaters on to warm the air so that when the cold refrigerant gas passed through the cooling coils from the compressor, the warmed moist air condensed on the coils. The condensate was collected and drained by a pipe out of the chamber in the same manner to standard air conditioners. This process occurred until the air was relatively dry, at which point heat from the air is transferred to the refrigerant gas in the coils. Thus, dehumidification always occurred before cooling.

However when very low air humidity levels were is required, an additional stand-alone dehumidifier became necessary. This type of equipment also utilised the same heat exchange principle using refrigerant gas. It warmed and cooled the air simultaneously. A MITSUI dehumidifier (Photo 10) which measures approximately 360mm x 350mm x 640mm was placed in the chamber. Its humidistat button, which controls the level of required dehumidification, was permanently turned to maximum. Power supply to the dehumidifier came from the PCO Unit, which regulated the frequency of dehumidification. Water removed from the dehumidifier was drained into a drainage pipe.

Photo 10 shows the MATSUI dehumidifier. Note the blue drainage pipe behind it.

### 3.1.8 Electric Fan

Air flow inside the climate-controlled chamber was produced a 560mm diameter cased axial fan that was driven by an 1100W electric motor (Photo 11). Power to the electric motor was regulated by a variable-speed drive unit that was located inside the electric distribution box. This variable-speed drive adjusted the frequency of the electric power supplying the fan motor from 25 to 50 Hz. Lower frequency power produced slow fan rotation and vice versa. The exact electric frequency for a required wind speed was determined by the PCO Unit using feedback from the wind velocity sensor (see later). Air flow from the fan assisted with air-mixing in the climate chamber and eliminated pockets of stagnation. The fan stood on four wheels, two of which are rotating clamp wheels. This allows the user to move the fan out of the way when warm Dummies are loaded into the middle compartment.

The fan was placed at a distance of approximately 400mm from the south wall of the chamber. This gap allowed enough space for large volumes of air to be drawn into the fan blades without putting strain on the electric motor. Air flow from the fan was directed towards the north wall through the middle compartment. At full speed appreciable air flow could be measured from every corner in the chamber, including the two side compartments. Wind generated by the fan produced a spiral vortex that gradually enlarged with increasing distance from the fan. Wind speed

measured at the periphery of the vortex was higher than that measured at the centre. This resulted in turbulence and excessive buffeting that was recorded as erratic measurements by the exquisitely sensitive velocity sensor (see later). In addition, the 1100W fan was just too powerful and easily exceeded the maximum recordable speed of 54 km/h by the wind sensor even at the lowest electrical frequency. Four layers of shade-cloth like material were placed behind the fan and used as a choke mechanism to address both of these problems. An extension sleeve of galvanised steel of ~30cm in length, with multiple blue PVC pipes of approx. 30mm diameter, was placed in front of the fan to provide some degree of forward-directed and laminar air flow to reduce the vortex effect

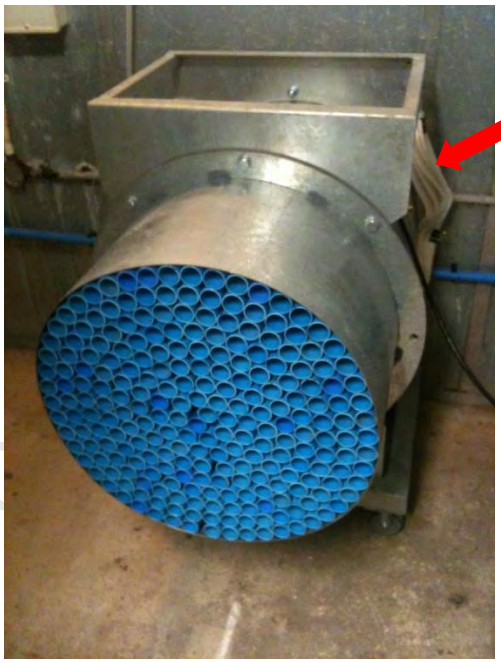

Photo 11 shows the 1100W fan. The left image shows the fan motor having 5 blades, and the image on the right shows the fan after the 30cm extension sleeve with multiple blue PVC pipes was fitted. Note the four layers of shade cloth attached behind the fan (red arrow).

### 3.1.9 Static Incubator

A wooden static incubator 750mm x 960mm x 650mm with a front-opening door was placed in the experiment monitoring room 2.01 (Photo 12). Its purpose was to warm Cooling Dummies. The incubator utilised 220V AC which, unlike the climate altering equipment in the chamber, was not connected to the PCO unit. However, two NTC thermocouple probes, each with a 144mm long spire, were placed in the incubator in order to monitor the core temperature of Cooling Dummies as they warmed (Photo 13). These thermocouple probes were connected to the PlantVisorPRO®. A third and stand-alone NTC thermocouple probe was placed in incubator to monitor its air temperature. The NTC probes both in the experiment chamber and in the incubator were manually calibrated to 0 ºC by being swirled in ice water.

Photo 12 shows the chicken-egg incubator in room 2.01 for warming Cooling Dummies

Photo 13 shows two NTC probes in the incubator.

Sensors for air temperature and relative air humidity are combined in a single unit that is manufactured by Carel (Photo 14). The combined sensor was mounted on a small insulated panel that was fixed to the floor in the middle compartment. The sensor measures relative humidity and temperature of the air that passes over the cooling Dummies. Measurements were relayed to the PCO unit by wire.



Photo 14 The CAREL combined air temperature and air relative humidity sensor unit placed inside the climate controlled chamber.

### 3.1.11 Air Velocity Sensor

The air velocity sensor was a 300mm long, horizontally mounted plastic rod that had a 10mm long slot on one end in which a metal plate is exposed to the air flow (Photo 14). The sensor was also mounted on the small insulated panel on which the air thermometer and relative air humidity sensor is mounted.



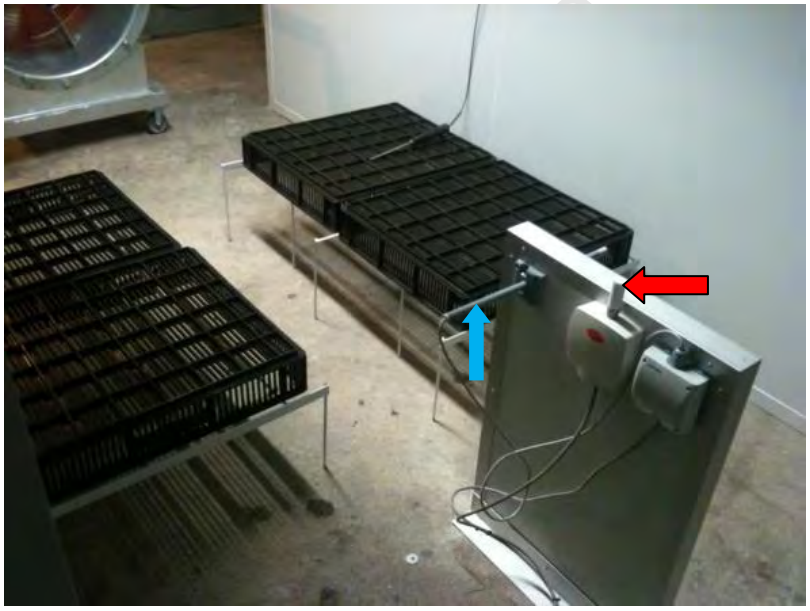

Photo 15 shows the combined air temperature and relative air humidity sensor (red arrow) and wind velocity sensor (blue arrow). Note the black plastic crates on which Cooling Dummies rest during a cooling experiment.

## 3.2 Cooling Dummies

Cooling dummies were validated as thermal manikins that adequately represent post-mortem cooling and utilised in numerous other studies of post-mortem cooling [35, 36, 37, 38, 40, 61, 62,]. The obvious advantage is that they could be re-used after cooling. In these studies cooling dummies were made by filling a soft rubberised container, usually natural rubber (caoutchouc) or a synthetic variant such as neoprene[62], with a special gel solution consisting of 47.5% distilled water, 47.5% glycerol and 5% agar. The special gel has similar thermal properties to human tissue and is elastic at temperatures below 40ºC [35]. After the gel set, the Cooling Dummy would be placed in an incubator and warmed to 37ºC. Heat withdrawal by its removal from the incubator would be regarded as the 'time of death'. The Cooling Dummy would be placed in an environment in which the ambient temperature $T_a$ would be kept constant, a thermometer would be inserted deep into the core and serial measurements of core temperature $T_c$ would be taken during the course of cooling. Temperature curves from such Cooling Dummies have a double-exponential shape and even a post-mortem temperature plateau similar to human bodies.

Two pairs of Cooling Dummies were made for this study project, each pair consisting of one large and one small Cooling Dummy. The idea of making two pairs was that for any given experiment a pair would be cooling during that

experiment in the controlled climate chamber while the other pair would be warming in the incubator, in preparation for the next experiment. At the end of each experiment the pairs would swop places. The thinking was that the process of warming of Cooling Dummies to 37°C takes time, and delays would result if the researcher was to wait for cold Dummies to warm.

The Cooling Dummies for this were made by filling neoprene diving suits with a special gel made by of a solution of 47.5% glycerol, 47.5% distilled water and 5% agar. Two size XS (extra small) diving suits for small females and two size JS wetsuits for children were bought. Agar powder and glycerol were bought from a local chemical supplier, and distilled water was obtained from University laboratories. A 20L aluminium pot, a gas stove, a mechanized hand mixer, a large wooden spoon and a 1 litre glass jug were bought from the local supermarket. To make a large Cooling Dummy, 9.5L of distilled water were poured into the pot on the stove, followed by 9.04L of glycerol. The two liquids were continuously stirred while being warmed by the gas stove, while the temperature was monitored by a handheld electronic thermometer to 80˚C. When the solution reached 80˚C one kilogram of agar powder was slowly poured into the pot. The mechanized hand mixer was used to dissolve the powder in the solution. After closing the shoulders and thighs of the wetsuits with cable ties, the viscous and hot solution was poured into the neoprene wetsuits through the neck opening. A small plastic bucket was

then placed in the neck opening and tied by a cable tie. The Dummy was then left to cool and set.

To make a small Cooling Dummy 3325 ml of distilled water, 3.16L of glycerol and 350g of agar powered were used in a similar manner. Final Dummy weights were 19.88kg, 15.83kg, 10.64 kg and 9.74kg. Weights of two large and small Dummies were obviously not identical as planned. This was because not all the thick gel-based solution could be practically poured from the pot into the wetsuits. Small amounts of the solution were either left in the pot and on the stirring spoon, and small amounts were inevitably spilled on the floor during pouring of the solution into the wetsuits. Small holes of approximately 20mm in diameter were cut at the groin of each wetsuit and clear Perspex straws were inserted towards to the core. NTC probes were to be inserted into these straws to measure core temperature when the cooling dummies would be both in the incubator and in the climate controlled chamber. Table 1 summarises weights and designated letters of the four cooling dummies.



| Designated Cooling Dummy Letter | Mass |
|---|---|
| A | 19.88kg |
| B | 10.64kg |
| C | 15.83kg |
| D | 9.74kg |

Table 1. Cooling dummy weights and designated letters.

During the course of the experiments, which was a little over 12 months, it was been observed that small amounts of precipitation had built up on the inner surface of the Perspex window of the static incubator. Sweet taste of this condensation suggested that it was glycerol which must have been evaporating from the 20mm incisions made at the groin of each Cooling Dummy, through which NTC probes were inserted. Closer inspection of all Cooling Dummies showed slight sagging of the wetsuit around wrinkles on the thighs that were made by the cable ties. This was an indication that perhaps water and glycerol from the special gel in the Cooling Dummies had slowly evaporating over time through the groin incision.

## 3.3 A Thermostatic Gel Manikin (TGM)

An excess of agar powder and glycerol had been left over after the four Cooling Dummies were made. The idea of making an internally self-warming Cooling Dummy was unrelated to this study project but was intended for private use to understand the clinical phenomenon called hypothermia after-drop, in which the core temperature of patients suffering from severe hypothermia continues to decrease despite active rewarming in emergency departments, after which death often follows[63, 64, 65]. Personal experience with working with the four Cooling Dummies over a period of ~1year hinted that perhaps similar heated transfer mechanisms were at play. The thermostatic gel manikin (TGM) was fabricated to verify this hypothesis. But it was equally applicable in this study: it would warm itself internally to 37ºC at the end of a cooling experiment so as to avoid the burden of carrying it back and forth from an incubator. However, the idea extended so that the self-heating Cooling Dummy could distribute internally-generated heat to its surface in a manner similar to the human circulatory system.



In addition to the special solution of distilled water, agar powder, glycerol and neoprene wetsuit mentioned earlier, this TGM consisted of:

- A cylindrical JBJ 800W True Temp® Titanium aquarium heater that consisted of a cylindrical titanium rod encased in glass; an electronic control/LCD unit normally used to monitor and control aquarium water

temperature that is located between the glass rod to a power plug, and a small thermometer probe normally used for water temperature measurement that connects to the glass rod. This aquarium heater was permanently embedded inside the TGM. It had a power rating of 800W, 240V A/C. The electronic controller unit was removed and replaced by a multi-range unequal repeating timer with which electric current was manually adjusted to pulsate using two dials: one to set the relay interval and the other to set time interval between relays. Removal of the native electric controller unit rendered the aquarium heater's native thermometer probe obsolete. A detachable connection was made in the aquarium heater's electric lead using a male-female electric coupler to facilitate easy moving of the TGM.

- A 2mm thick wire frame was fashioned into the shape of a small female torso without arms and legs. The wire was epoxy-coated to reduce thermal conductivity. The wire frame formed a skeleton to provide a realistic representation of the shape and rigidity of a human torso, as well as provide attachment points for the JBJ 800W True Temp Titanium heater and its thermometer probe, the polyurethane pipes and an negative temperature coefficient (NTC) probe for measuring the core temperature (Photo 16).
- A 50mm long NTC probe was placed in the centre of the TGM in close proximity to the aquarium heater's glass rod for measuring the core temperature. The NTC probe's electric lead exited the TGM through the

neck and connected to the PlantVisorPRO® for data logging via a coupler that would facilitate easy moving of the TGM. It is this NTC probe that was used for manually regulating electric supply to the aquarium heater after the native temperature probe of the aquarium heater was rendered obsolete by removal of the native electronic controller.

- A circulatory system consisting of an internal and external component:
  - The internal component was placed within the TGM itself and consisted of clear and blue polyurethane piping, both having a 10mm external diameter and an 8mm internal diameter. Clear polyurethane pipe represented the peripheral circulation and was attached in a spiral fashion to the outside of the wire frame using cable ties. The blue coiled polyurethane pipe was placed around both the JBJ 800W True Temp® Titanium heater and core temperature NTC probe and was joined to the clear polyurethane pipe by a connector. Both the clear and blue polyurethane pipes exited the TGM at the neck, where they terminated. Each was connected to a ball-valve connector to facilitate easy detachment of the TGM from external component of the circulatory (see below) when necessary.
  - The external component of the circulation consisted of two short lengths of clear polyurethane pipe that both connected to a single electric diaphragm fluid pump, one in the inlet and the other in the outlet of the

pump. The external clear pipes connect to the already-mentioned ball-valve connectors of the blue and clear polyurethane pipe coming from the neck of the TGM, respectively, thus completing a closed circuit. Each external clear polyurethane pipe was insulted with 6.5mm flexible rubber foam tubing.

- The electric diaphragm pump formed part of the external circulation and was connected to a power supply of 220V A/C via a DC transformer that produced 24V, 0.56A. The electric diaphragm pump was insulted by 20mm thick flexible rubber foam tubing. The pump's open-flow pump rate was 1L per minute and maximum pressure was 324PSi. The total volume of the circulatory system was 500ml. The cycle period in the closed system was 30 seconds.
- The last component of the circulatory system was the circulating fluid itself, for which 2.77mol/$l^{-1}$ of sodium chloride (NaCl) solution was used. This concentration has a specific heat capacity of 3604 $Jkg^{-1}$ $°C^{-1}$, which is nearest to that of human whole blood of 3594 $Jkg^{-1}°C^{-1}$ compared to normal saline, distilled water, Hartman's solution and Gelofusin [66]. The circulation was under the surface of this solution after all gas bubbles were allowed to escape.
- Twenty litres of the special agar/glycerol/distilled water solution, as per previous recipe, were used to make the TGM.

The final mass of the complete TGM was 20.93kg (Photo 18), maximum width 550 mm from shoulder-to-shoulder, 160mm front-to-back and 480mm from groin to neck base.

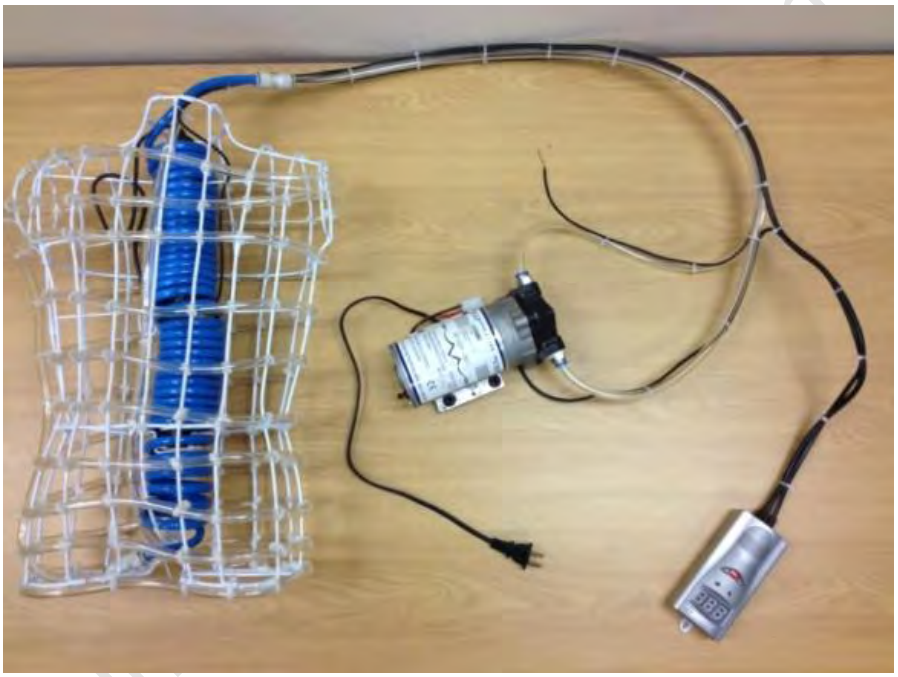

Photo 16 Shows the TGM's white epoxy-coated wire frame to which clear polyurethane pipe is attached, blue polyurethane pipe in the core surrounding the titanium aquarium heater (not visible), external clear polyurethane pipes connected to the electric diaphragm pump, and the native temperature control unit/LCD of the aquarium heater (later replaced by adjustable timer).


Photo17 shows the neoprene wetsuit whose arms and legs were cut off and internally stitched.


Photo 18 shows the fully developed TGM. Note the blue and clear polyurethane pipes, electric lead and NTC lead all exiting at the neck.

## 3.4 COOLING EXPERIMENTS

Cooling experiments were divided into two phases:

### 3.4.1 Phase 1 Cooling Experiments

Phase 1 cooling experiments were scheduled experiments using the four standard cooling dummies. Cooling experiment were scheduled such that two of the three variables (air temperature, air humidity, wind velocity) whose effect on cooling rates were to be studied were kept constant while one was changed at small increments for each experiment from a low value over a defined range to a high value. The process was to repeated for each variable in turn. Because the four Cooling Dummies had different weights, a pair consisting of a large and small cooling dummies could not be substituted for another; therefore all four had to undergo the same cooling experiment. The total number of experiments to be completed depended on the magnitude of increments by which the each variable under investigation would be changed. For example, because there were three variables under investigation, i.e. wind speed, air temperature and relative humidity, the total number of experiments to be conducted for a mere three increments of 33.33% for each variable required 27 (which is $3^3$) experiments for each cooling dummy pair, or 54 for all four cooling dummies.

Before each experiment a pair was placed in the incubator and warmed to 37ºC, after which it was placed on the plastic crates in the climate controlled chamber (Photo 15). The two pair alternated in this routine. During experimental cooling, core temperature measurements from the two Cooling Dummies in the climate controlled chamber were logged by the PlantVisorPRO®, while core temperature measurements from the other pair in the incubator were also being logged simultaneously.

### 3.4.1 Phase 2 Cooling Experiments

Phase 2 cooling experiments were not part of the original experiment schedule but were carried out using the TGM, which itself was fabricated during Phase 1, after Cooling Dummy C was unexpectedly retired due to unsatisfactory performance. Phase 2 cooling experiments A total of four experiments were carried out using the TGM.

i. Experiment 1 was carried out to obtain a baseline cooling curve of the TGM to determine whether its cooling curve was comparable to those of the standard cooling dummies. In the first experiment the core of the TGM was warmed from 20ºC to 37ºC over a period of 1320 minutes. Thereafter the GTM was transferred from the incubator and placed in the climate-controlled laboratory at 21.1 ºC in under 20 seconds.

ii. After the core of the GTM had cooled to 21.1ºC Experiment 2 was carried out under identical ambient conditions, but in which the internal aquarium heater had been switched on to increase core temperature to 37ºC. When the core temperature reached 37ºC the internal aquarium heater was switched off and temperature measurements of subsequent core cooling were made.

iii. Use of the internal heater in a cooling dummy in Experiment, which appears to be the first of its kind, yielded unexpected result that demanded further investigation that necessitated two additional unscheduled experiments in the form of Experiment 3 and Expedient to be carried out. Results of Experiment 2 and these additional two experiments are discussed under the appropriate chapter.

# CHAPTER FOUR

# RESULTS

A total of 23 experiments were completed successfully and are summarised in Table 2.

| No | Cooling Dummies | Air Temp | Relative humidity | Wind Speed | Time | Comment |
|---|---|---|---|---|---|---|
| 1 | C | 10 | 100 | 0 | | Test run |
| 2 | A & B | 20 | 50 | 0 | 26hrs | Excess precipitation from Exprt. 1 on walls/floor |
| 3 | C & D | 20 | 100 | 0 | 16hrs | Condensation on cooling dummies |
| 4 | A & B | 10 | 100 | 0 | | Mist formation in chamber |
| 5 | - | - | - | - | - | Aborted, RH remained high from Exprt. 4 |
| 6 | C & D | 20 | 54 | 10 | 17hrs | Sensitive velocity sensor → fluctuant curve |
| 7 | A & B | 20 | 54 | 10 | | |
| 8 | C & D | 20 | 54 | 20 | | |
| 9 | A & B | 20 | 54 | 30 | | |
| 10 | C & D | 20 | 54 | 30 | | |
| 11 | A & D | 20 | 54 | 40 | | |
| 12 | C & D | 0 | 54 | 40 | | |
| 13 | A & B | 0 | 67 | 40 | | |
| 14 | C & D | 0 | 78 | 0 | | |
| 15 | A & B | 20 | 50 | 20 | | |
| 16 | C & D | 20 | 45 | 10 | | |
| 17 | A & B | 20 | 37 | 10 | | |
| 18 | C & D | 20 | 18 | 0 | | |
| 19 | A & B | 20 | 20 | 0 | | |
| 20 | A & B | 20 | 20 | 10 | | |
| 21 | C &D | 20 | 18 | 50 | | High wind affected RH sensor |
| 22 | A & B | 20 | 17 | 50 | | |
| 23 | C & D | 20 | 50 | 20 | | Unexpected failure of Dummy C. Disregarded. |
| 24 | TGM | 21.1 | - | 0 | | Test run, incubator warming. RH sensor off. |
| 25 | TGM | 21.1 | - | 0 | | Test run, internal warming |
| 26 | TGM | 21.1 | - | 0 | | Repeat of Exprt 24 with surface temp sensor |
| 27 | TGM | 21.1 | - | 0 | | Repeat of Exprt 25 with surface temp sensor |

Table 2. Showing cooling experiment schedule. The first 23 experiments make Phase 1 and the last four experiments highlighted in green make Phase 2.

4.1 Experiment 1 was the first cooling experiment preformed in the climate-controlled laboratory using Cooling Dummy C. The RH was set to100%, the room temperature set to 7.5°C and wind velocity set at 0km/h. The achieved room temperature was 10°C due to the heat of the steam from the humidifier that was being continuously produced to maintain 100% RH. The RH in the experiment chamber took three hours to be maintained at high levels of between 90% and 95%. The purpose of this experiment was to test the cooling characteristics of this dummy, as well as the behaviours of the different hardware involved in the experiment. The cooling curve from this experiment exhibited the expected characteristics as described in the literature, namely a double-exponential sigmoid curve with an initial plateau during which the core temperature does not decrease, followed by a rapidly accelerating rate of cooling, followed by a progressively slowing rate of cooling until the core temperature equals the ambient air temperature. During this experiment it was noted that the incubator temperature set point needed to be at 38 ºC in order for the cooling Dummies to reach core temperatures of 37.2 ºC.

4.2 Experiment 2 took approximately 26 hours to complete. The RH fluctuated between 50% and 70% despite a dehumidification demand of 100%, i.e. the room RH was set to 0%. This 'failure' to dehumidify as expected was attributed to excess water in the wall panels and floor of the experiment chamber from the previous experiment. During this experiment Dummies C and D took approximately 16 hours to warm from 20 ºC to 37 ºC.

4.3 Experiment 3 took approximately 16 hours to complete. At the end of the experiment the Dummies C and D were wet to touch due to condensation. This was thought to be responsible for the extremely rapid rate of cooling in comparison to Experiment 2 conducted the previous day.

4.4 In Experiment 4 there was mist formation in the experiment chamber when the humidifier was on which lasted approximately 10 minutes, followed by another 10 minutes of no mist.

4.5 In Experiment 5, which was aborted, the RH remained high and refused to reduce for a scheduled experiment, despite the RH set point being at 50%. Instead the over-heat safety switch of the compressor on the ground floor tripped without giving a warning to that effect. The result was that no cooling occurred in the climate-controlled chamber. The switch had to be manually rest. Meanwhile the walls and floor of the climate-controlled chamber were visibly moist. In an attempt to evaporate water from the floor and walls of the experiment chamber the room temperature was set at 40 ºC.

It was left baking for three days. Thereafter the climate controlled chamber door was opened for 6 minutes and the RH dropped from 45% to 20%. After this incident the decision was taken to postpone all high RH experiments for last. The next set of experiments would be of increasing wind velocity at low room temperatures and low RH.

4.6 Experiment 6 took approximately 17 hours to complete. The wind curve on the PantVisorPRO® appeared to be highly fluctuating with readings of between 0 km/h and 24km/h. These fluctuations occurred over very short periods of time and were due to buffeting as a result of the high sensitivity of the wind velocity sensor. The recorded average wind speed was, however, exactly 10.0km/h which sufficed for purposes of the study.

4.7 Experiment 7 occurred without incident. Set points of this experiment were not changed from the previous experiment.

4.8 Experiment 8 was identical to Experiment number 7, with the exception of the wind speed being 20 km/h.

4.9 Experiment 9 was conducted successfully without incident.

4.10 Experiment 10 was conducted successfully without incident.

4.11 In this experiment number11, despite the RH set point being 10%, the achieved RH in the climate chamber was an average of 52% and we couldn't find an explanation for this because the concrete floor of the experiment chamber appeared dry.

4.12 In this Experiment number 12 the room temperature set-point was 0ºC. Despite the RH set-point being 10%, the achieved RH was an average of 54% and we couldn't find an explanation for this because the concrete floor of the experiment chamber appeared dry.

4.13 In this Experiment number 13 the RH set point was 10% but the actual achieved RH was an average of 67%. We couldn't find an explanation for this because the concrete floor of the experiment chamber appeared dry.

4.14 In this Experiment number 14 the humidity functionality of the experiment chamber was switched off so that the recorded RH was natural. In effect this experiment was only to obtain cooling curves of Dummies C and D at 0ºC.

4.15 Experiment 15. The original door seal of the experiment chamber was made from leather and had dried and become brittle over the many years after it was put in, resulting in the chamber door being leaky of air humidity. A new rubber seal was put in place and low RH could be achieved once again. In retrospect this was the reason for uncontrollable RH levels for Experiments 11, 12, 13 and 14.

4.16 Experiment 16 was conducted successfully without incident.

4.17 Experiment 17 was conducted successfully without incident.

4.18 Experiment 18 was the first low-RH experiment for Dummies C and D.

4.19 Experiment 19 was the first low-RH experiment for Dummies A and B.

4.20 Experiment 20 was conducted successfully without incident.

4.21 Experiment 21 saw the curve of RH in the climate chamber becoming irregular due to high wind velocity of 50 km/h which affected the RH sensor.

4.22 Experiment 22 was the first high wind-velocity experiment at low RH. The RH curve at this wind speed was noted to be slightly irregular, but otherwise all went well.

4.23 In Experiment 23 the cooling curve of Cooling Dummy C had an unexpected single sinusoidal shape with no usual PMTP. The cooling curve of the 9.74kg Cooling Dummy showed an unusual slowed response where, after probe insertion, core temperature rise slowed before the maximum core temperature measurement was made. This was in contrast to previous experiments where the core temperature measurement would be instantaneously rising from the ambient to 37ºC at the insertion of the probe, resulting in a vertical curve. This experiment was abandoned and results not incorporated. Instead the TGM was used.

4.24 In Experiment 24: The aim of this experiment was to assess and compare the core cooling curve of the TGM with those of the other Cooling Dummies. In this experiment the TGM was disconnected from the external circulation, with NaCl solution still in the internal circulation, and was placed in the incubator. Its core temperature was raised to 37.2ºC in the regular manner.

The time-curve of the core temperature is illustrated in Fig. 1. There is an interval of precisely 60 minutes between the connection of the core NTC probe and the first change in the core temperature that is regarded as being the PMTP.

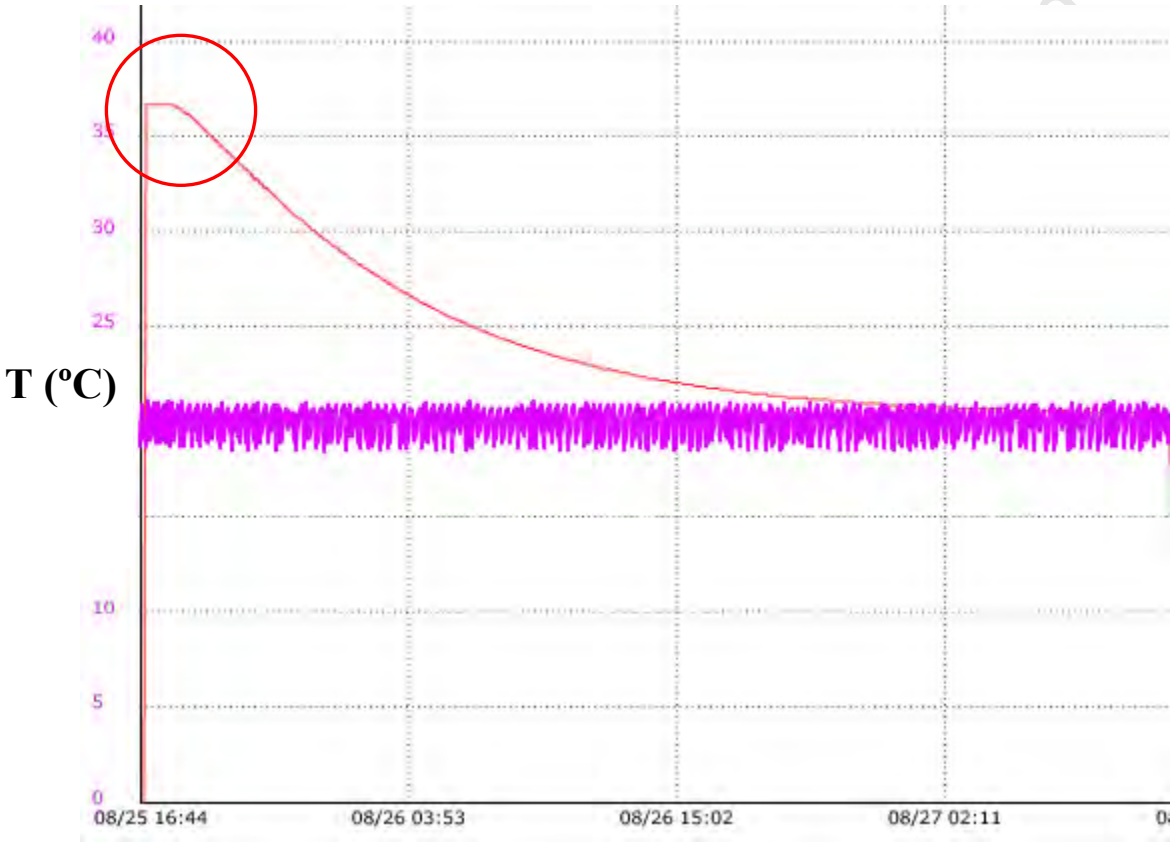


Fig 1 illustrates core temperature curve of the TGM as it cooled in ambient temperature of 21.1ºC. The red circle highlights the PMTP.

After the flat PMTP the curve in Fig.1 illustrates a brief and transient interval in which the rate of core cooling gradually increases, prior to the practically straight part of the curve that represents the maximum rate of cooling. This transient interval falls outside of the definition of PMTP as discussed earlier and its nature is discussed later in the paper. After the steepest part the curve tapers as the core temperature approaches the ambient temperature. The time-temperature curve from Experiment 24 thus has a double-exponential shape as described in the literature and as such the TGM was accepted to cool as a typical cooling dummy was to be expected. Insertion of an internal core heater, which is a deviation from the conventional recipe of making cooling dummies, did not affect cooling of the TGM. The core temperature in Experiment 24 took ~1440 minutes to reach 21.1ºC.

4.25 Experiment 25: The purpose of this experiment was to assess cooling characteristics of the TGM core after internal heating. The TGM was placed in the climate-controlled chamber at 21.1ºC. After the core of the GTM had cooled to 21.1ºC the internal aquarium heater had been switched on to increase core temperature to 37ºC. When the core temperature reached 37ºC the internal aquarium heater was switched off and temperature

measurements of subsequent core cooling were made. Fig. 2 illustrates the core temperature $T_c$ time cooling curve.



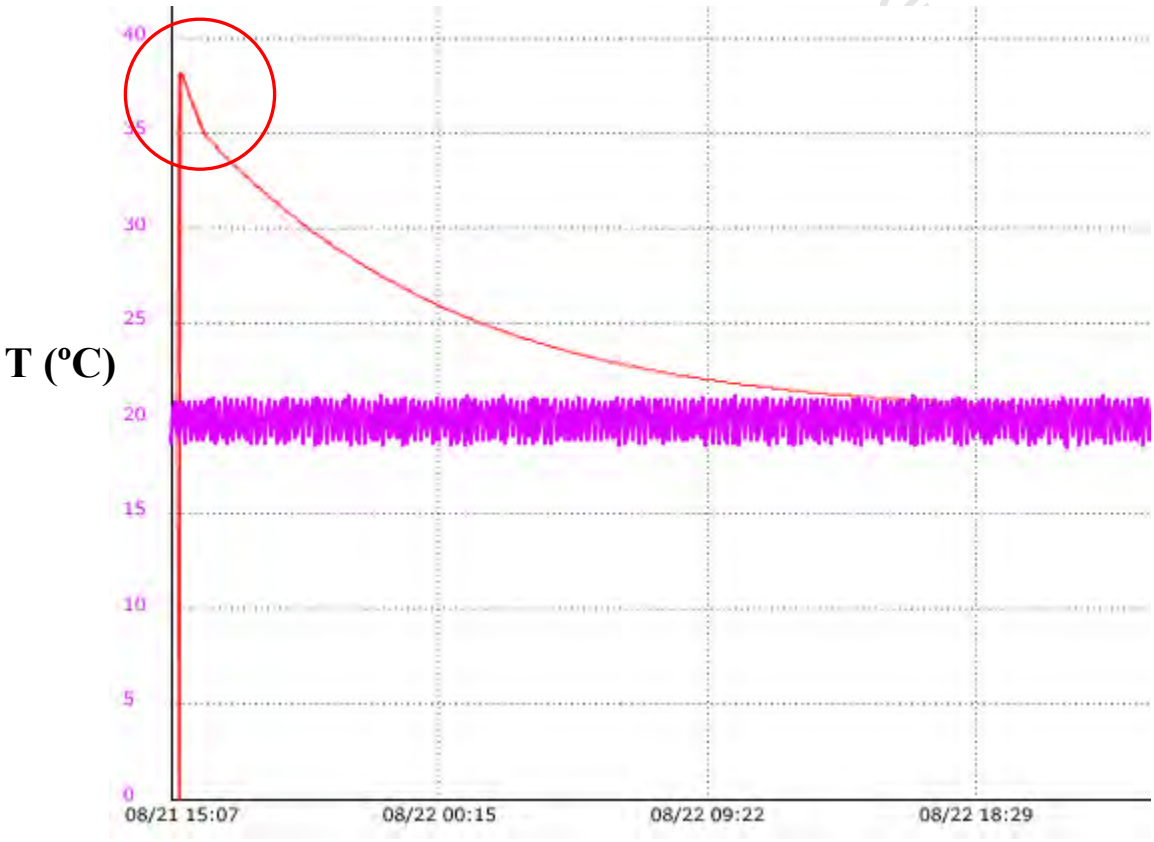


Fig 2 illustrates the core temperature curve of the TGM after internal core warming using the aquarium heater. Red circle highlights normal position of the PMTP.

In the time-temperature curve from Experiment 25 illustrated in Fig. 2 there is no PMTP despite the fact that the ambient temperature, core temperature and all other known factors that are usually considered in cooling studies and when calculating the post-mortem interval were kept identical to those of Experiment 24. In fact the rate of core cooling is at a maximum in the very part of curve where one would ordinarily expect to find the PMTP. The shape of the cooling curve from this experiment is a single rather than double-exponential. The reason for this discrepancy was revealed after a second NTC probe was attached onto the anterior surface of the TGM to measure surface temperature $T_s$, followed by repetition of Experiments 24 and 25.

4.26 Experiment 26: This experiment is the repeat of Experiment 24 but in which the surface/skin temperature $T_s$ was also measured, see Figure 3. The temperature-time curve of the core from this repeat experiment is identical to that of Experiment 24. The temperature-time curve of the surface shows an extremely rapid rate of cooling from 37ºC immediately after heat withdrawal, which occurs while the core temperature remains unchanged during the PMTP. Rapid surface cooling thus establishes a temperature gradient between the core and the surface that had been zero at the time of

heat withdrawal when the core and surface temperatures were equal. The surface temperature curve in Fig. 3 then shows a decreasing rate of cooling as a single exponential curve approaches the ambient temperature at the same time as the core temperature.

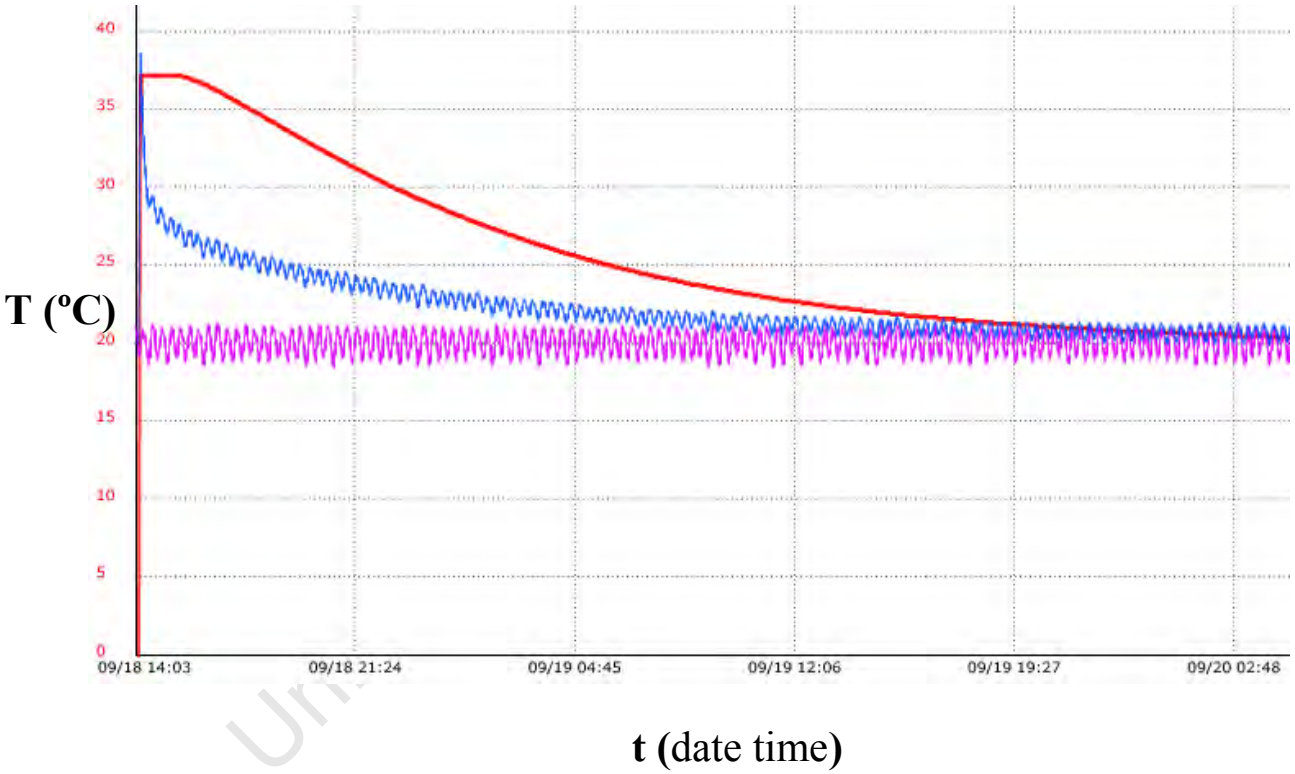


Fig. 3 illustrates the surface temperature curve (**blue**) from Experiment 26 together with the core temperature curve (**red**).

4.27 Experiment 27: This experiment is a repeat of Experiment 25 but in which a surface NTC probe is attached and is illustrated in Fig. 4. The black arrow indicates the instant when the internal aquarium heater was switched off ($t_0$), at which time the average surface temperature was 21.6ºC. As was to be expected, the time-curve of the core temperature is identical to that of *Experiment B*.

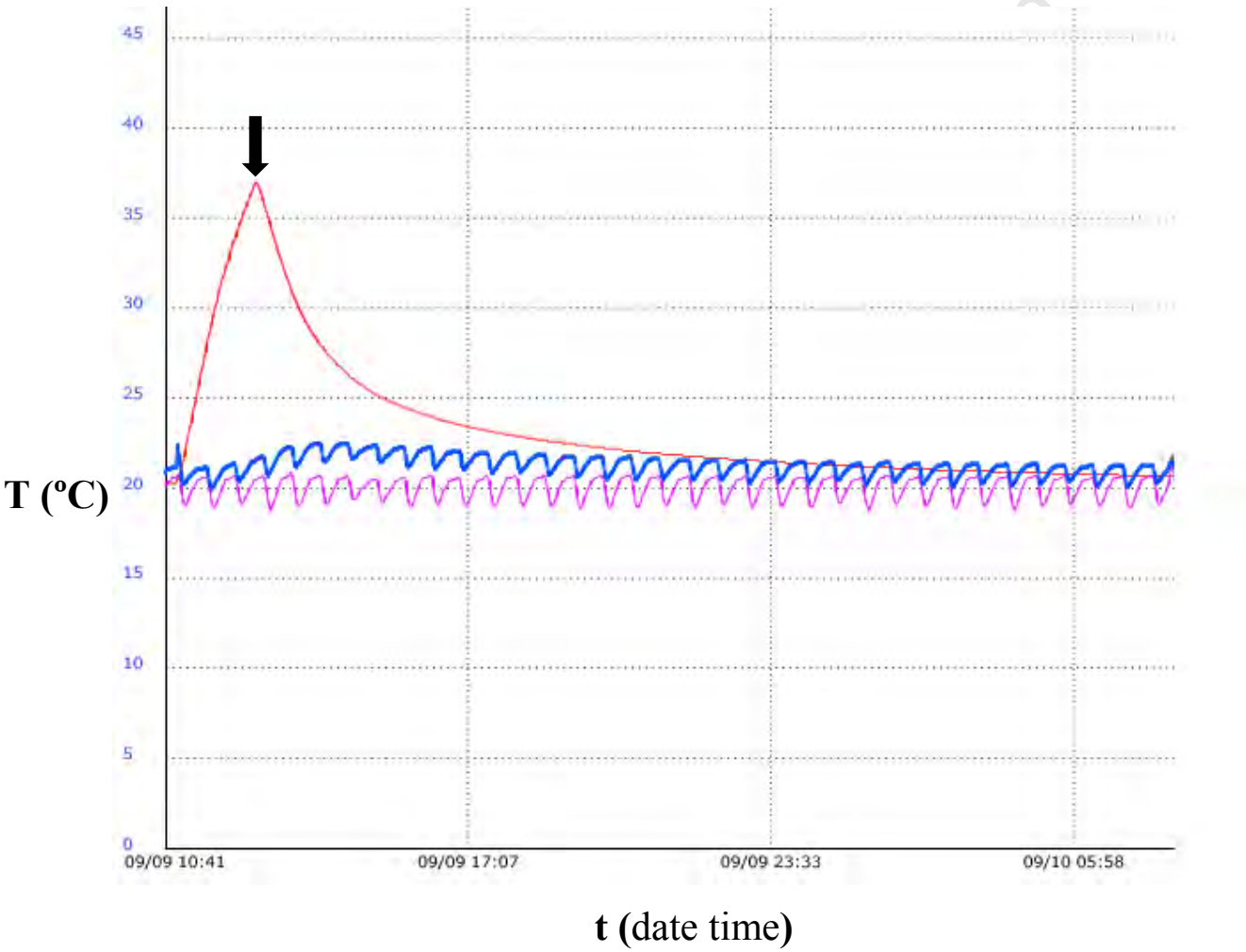


Fig 4 illustrates Experiment 27. Core temperature (**red**) increased rapidly while surface temperature (**blue**) increased gradually temporarily. Black arrow = internal heater switched off ($t_0$).

# CHAPTER FIVE

# DISCUSSION

The difference in shape between core cooling curves from Experiments 24 and 25 proved to be the turning point of the entire study project that brought the experiment schedule into a sudden halt. Absence of the PMTP in the first part of the curve when the internal heater was used, where instead the curve was steepest, was totally unexpected. There was no adequate explanation for this observation in the Nomogram method, its mathematical expression or its original predecessor, the Cooling Formula by Marshall and Hoare. All parameters considered in the Nomogram method were kept identical in the two experiments, i.e. the core and ambient temperatures were identical, and there was no explanation of how the internal heater experiment changed the value of the correction factor $f$ used for the calculating the cooling constant $Z$. All exclusion criteria in which Henssge stated that the Nomogram method should not be used [1] were carefully excluded. The difference in the shape between the two cooling curves therefore suggested that there was another factor at play which the Nomogram method did not consider.

When the internal heater in Experiment 27 was switched off the surface temperature was 21.6ºC. This meant that a difference in temperature of 15.4ºC between the surface and the core was already well-established at $t_0$. It is this difference that was thought to result in the extremely rapid rate of core cooling seen after the heater was switched off. The cold bulk of the body mass around the warm core was thought to have absorbed and dissipated heat radially away from the core. Cooling of the core, in turn, resulted in a decrease of the temperature difference between the surface and the core over time, the latter process itself resulted in decreasing rates of subsequent core-cooling. Heat that was concentrated at the core at $t_0$ dissipated and spread out to the entire body, getting weaker closer to the surface and resulting in a slight rise of the surface temperature as seen on Fig 4.

From these experiments two crucial observations were made:

- The rate of core cooling depended not on the excess between core and ambient air temperatures, as is the traditional belief, but depended directly on the excess between core and surface temperatures, or CSTG. It was the magnitude of this temperature excess at the time of heat withdrawal, rather than the individual values of $T_c$ or of $T_s$, which determined the core cooling rate, and

- The PMTP was present when the CSTG was equal to zero at the instant of heat withdrawal but it was not present when the CSTG was equal to 15.4ºC at the instant of heat withdrawal. Because it had earlier been observed that the rate of core cooling depended on the magnitude of the CSTG that is created on the surface, the apparent paradoxical observation in Experiment 26 that the core did not begin to cool as soon as the CSTG was no longer zero, i.e. the PMTP, was thought to be the result of a delay in propagation of the CSTG itself from the surface of the body to the core.

From these two observations the author formulated what is termed the *Core-surface Temperature Gradient Wave Propagation Hypothesis* to explain in detail the process to total-body cooling.

## 5.1 The Core-Surface Temperature Gradient Wave Propagation Hypothesis

The CSTG wave propagation hypothesis states that:

*"When the surface of a cylindrical or spherical solid body of uniform temperature distribution experiences a rapid temperature change such as cooling at the time of death, a temperature gradient is established between that surface and a layer of body immediately deep to it whose temperature is equal to that of the core – the internal temperature gradient. At the same time the said layer is exposed to an external temperature gradient between itself and the surface. The numeric difference between the internal and external temperature gradients is equal to the numeric difference between the core and surface temperatures and is referred to as the core-surface temperature gradient, CSTG. It is this CSTG that governs the rate of temperature change of the said body layer. Cooling of that layer, in turn, establishes a temperature gradient between itself and a deeper layer of body whose temperature is still equal to that of the core. The deeper layer is thus also exposed to two temperature gradients whose numeric difference is equal to the CSTG, and it also cools as a result. Cooling of successive layers of body between the surface and core occurs in a similar manner. Therefore this CSTG physically propagates away from the surface on which the initiating temperature change occurred and causes temperature change in successive layers of the body as it propagates. The propagation rate of the CSTG is inversely proportional to thermal resistivity of the*

*body, which remains geographically constant for the duration of cooling. A human body has high thermal resistivity so that there is a delay in propagation of the CSTG to the core, resulting in the well-documented phenomenon of the PMTP that is also observed in cooling dummies. The duration of the PMTP is directly proportional to the distance of the core (point of temperature measurement) from the surface: all else being equal, the further away the core is from the surface, the longer the CSTG propagation interval will be, and hence the longer the PMTP will also be. The duration of the PMTP is also directly proportional to the body's thermal properties between the surface and the core: a body with infinitely-high thermal resistivity will have an infinitely-long PMTP, i.e. its core will never cool.*

*At any given layer of the body the magnitude of the CSTG first increases as rapidly as the rate of initial cooling of the surface, which occurs against a constant core temperature before the CSTG reaches the core. Once the core begins to cool, the magnitude of the CSTG at any given part of body begins due to simultaneous cooling of the core and surface, albeit at different rates. Any part of the body during the cooling interval thus experiences a wave-like CSTG that has high initial amplitude – hence use of the term 'wave'. The result of this wave propagation through the body is that different parts cool at different rates at different times. The shape of the core-cooling curve is thus determined by (i) the magnitude of the CSTG at the beginning of cooling, (ii) factors affecting the rate of surface cooling,*

*(iii) thermal properties of the inner body between the surface and the core, (iv) depth of thermometry in relation to body radius, and (v) the temperature excess between the initial surface temperature and ambient temperature, which determines the 'height' of the cooling curve when plotted on a time scale.*

*The initially slow rate at which the core's temperature responds to the arrival of the CSTG wave is a consequence of the core's thermal properties. The subsequent maximum rate of core-cooling, represented by the steepest and practically straight part of the curve, is the result of the maximum amplitude of the CSTG being at the core. The subsequent decreasing rate of core-cooling, represented by the last part of the cooling curve, is the result of the decreasing CSTG magnitude with time. When core and surface temperatures equal one another at the end of cooling, the magnitude of the CSTG becomes zero and subsequently the rate of cooling also becomes zero.*

*Factors that accelerate or decelerate the rate of surface cooling after CSTG wave propagation commences, such as changes in ambient temperature or changes in thermal conditions at the surface, merely create a secondary CSTG wave at the surface whose amplitude is equal to the temperature excess between the resultant surface temperature and whatever the core temperature at that time would be. Such secondary CSTG wave would also propagate towards the core at the same rate as the initial CSTG in accordance with the body's thermal resistance,*

*irrespective of its amplitude. Change of the rate of core cooling as a result of a secondary CSTG wave occurs after a period exactly equal to the PMTP."*

The CSTG Wave Propagation Hypothesis, which in the subsequent sections is also referred to simply as 'the hypothesis', is a unifying theory that satisfactorily explains total-body post-mortem cooling. It is attractive because it explains the discrepancy in initial core-cooling rates observed between Experiments 24 and 25. Although most authors agree that the post-mortem temperature plateau is the result of a temperature gradient being 'established' during cooling, very little explanation has been offered about the dynamics involved in that process. The term '*establishment of a temperature gradient*' has been used rather loosely by many authors without much elaboration, with a few exceptions. This dissertation describes for the first time that the said '*establishment of a temperature gradient*' actually refers to physical propagation of a wave of core-surface temperature gradient – established at the surface of the body due to rapid initial cooling of the surface – from the surface to the core, and this dissertation also demonstrates that such propagation results in the post-mortem temperature plateau and thus the double-sigmoid shape of the post-mortem core cooing curve. The obvious fact that the core does not cool directly to the external environment but first to skin is also emphasised for the first time in this paper. Implications of the hypothesis on

considerations that affect approach to thermometric thanatochronometry are discussed.

## 5.2 Characteristics of CSTG Wave Propagation

The CSTG wave propagation can be thought of as a single thermal 'shock-wave' that occurs when there is a change in temperature in any part of the body. When temperature change occurs on the surface, the wave propagates perpendicularly away from the surface. Because the wave is a temperature gradient that propagates through a solid body by thermal conduction, temperature change in a given part of the body occurs only when the wave reaches that part in accordance with Fourier's Law, which states that the time rate of heat transfer through a material is proportional to the negative gradient in the temperature and to the area, at right angles to that gradient, through which the heat is flowing. Fourier's Law is expressed mathematically as:

$$\overrightarrow{q_r} = -\lambda \frac{dT}{dt} \tag{5}$$

where $\overrightarrow{q_r}$ is heat flux (W/m$^2$) in the positive direction, $\lambda$ is the thermal conductivity of the body (W/mK) and $dT$ is the temperature gradient in the negative (opposite) direction to heat flux as indicated by the minus sign on the right hand side of the equation. What is important to note is that the temperature gradient $dT$ is between the core and the surface (and not the ambient environment)

through which heat transfer occurs by thermal conduction. Rearranging equation (3) gives:

$$\frac{dT}{dt} = -R_\theta \overrightarrow{q_r} \tag{6}$$

where $R_\theta$ is the thermal resistance of the material. Equation (6) can be regarded as a mathematical expression of the CSTG wave. The perpendicular/radial direction between the surface and core in a cylinder of infinite length is denoted by the subscript $r$. The propagation rate of the CSTG wave is determined by thermal resistance of the body, which is the inverse of thermal conductivity. The CSTG wave propagation exhibits both thermal and wave characteristics. Refraction of the wave occurs at a boundary of change of thermal resistance, resulting in change of velocity and/or direction.

The amplitude of the GSTG wave is determined by three factors:

(i) The rate of surface cooling occurring during the PMTP,

(ii) Thermal resistance between the surface and the core, which determines how quickly the effect of surface cooling from that given rate is transmitted to the core, and

(iii) The distance between the surface and the core, which determines the duration in which the given rate of surface cooling has an effect before core cooling begins, which itself determines the lowest possible surface temperature before the core cools.

Thus, a combination of rapid surface-cooling, high thermal resistance between the surface and the core and a large distance between the surface and the core, i.e. radius, results in very large wave amplitude and a very long PMTP. In an isotropic medium, such as the specialised solution used to make cooling dummies, the propagation rate of the CSTG wave remains constant. The CSTG wave has an asymmetrical single-sinusoidal shape as illustrated in Figure 5, which is due to very rapid surface cooling after heat withdrawal during the PMTP. As mentioned before, the peak or amplitude of the wave is created in the early cooling interval before other parts of the wave are created, so that during wave propagation the peak travels ahead of the rest of the wave.



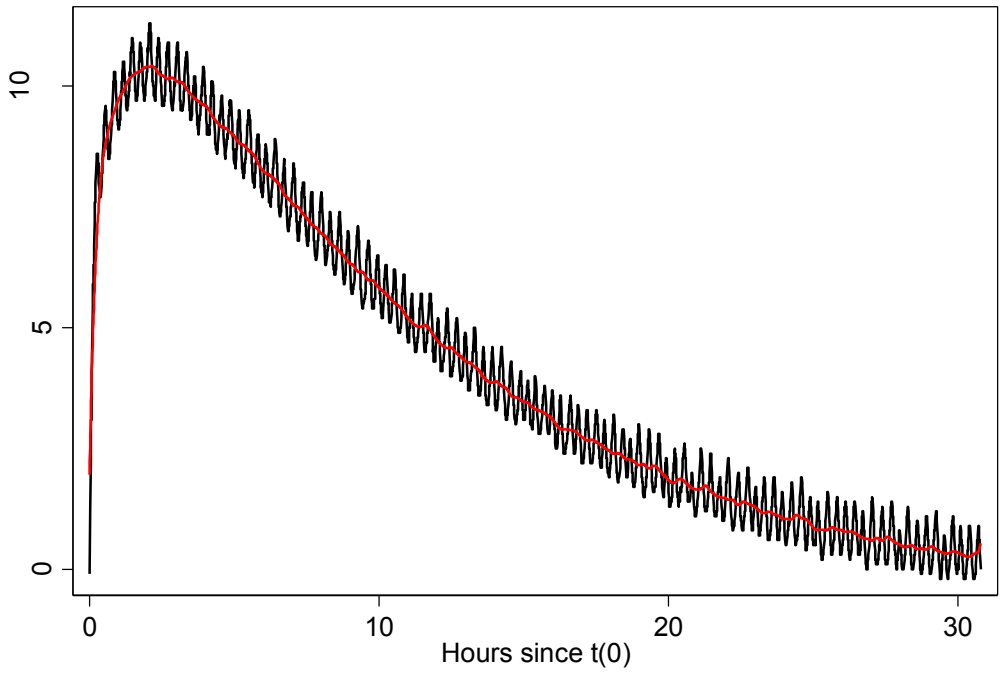


Fig 5. The CSTG curve from Experiment 26 plotted over the cooling interval. The trend line is in red.

The single sinusoidal shape of the CSTG curve over the cooling interval is similar to that shown by Schwarz and Heidenwolf [9]. However, Schwarz and Heidenwolf did not appreciate the propagative nature of the CSTG. On the other hand, Sellier [16] did describe a 'wave propagation' of a temperature gradient, but was not explicit or emphatic that it was between the core and the surface. Had these authors collectively realised that they were referring to the same phenomenon, they likely would have described the hypothesis. The fact that during the PMTP there is a measurable CSTG despite absence of core cooling makes it difficult to appreciate that the rate of core cooling is directly proportional to the magnitude of the CSTG. But once this relationship is appreciated it is easy to conclude the cause of the PMTP.

Arrival of the amplitude of the CSTG wave at the core marks the end of the PMTP and marks the beginning of core cooling. The core suddenly experiences a large temperature gradient between itself and the surface, which develops rapidly over a very short time to reach maximum amplitude. The result is that the rate of core-cooling also accelerates from being zero to being a maximum immediately after the PMTP, as represented by the practically straight part of the curve that has the steepest gradient. Transition from the PMTP to the maximum rate of cooling is not abrupt or instantaneous but is characterised by a brief and gently sloping part of the

time-temperature curve between the PMTP and the practically straight part, which is a function of the inner body's thermal resistivity.

The amplitude of the CSTG wave at the core gradually decreases with time as the wave propagates 'past the core', resulting in a corresponding decrease in the rate of core-cooling in the late stages. The length of the entire cooling interval is determined by the rate of propagation of the CSTG wave through the body, which itself is determined chiefly by the body's thermal resistance, among others.

The CSTG propagation hypothesis is a departure from Joseph and Schickele [26] description the initially slow rate of core cooling which they attributed to a small temperature gradient existing at the core: the hypothesis attributes it to thermal resistivity of the core despite to the arrival of a high CSTG amplitude.

## 5.3 Implications of the CSTG Wave Propagation Hypothesis

The fortuitous description of the CSTG Wave Propagation Hypothesis within the context of this study project provided a new level of understanding of total-body cooling that had not been described in the previous literature, which has multiple implications on how thermometric thanatochronometry should be approached. The hypothesis brings together multiple factors, some of which have been considered by previous authors, some of which have not been considered, and some of which have been considered in isolation. Previous understanding of how such factors interact may be responsible for the varying levels of success of many mathematical models applied in thermometric thanatochronometry. The diversity of these factors, their cumulative but interconnected nature, natural evolution and progress of thermometric thanatochronometry methods over the years and the understandable pursuit of user-friendly or mathematically simple but acceptably accurate methods all make the aesthetic dissection and presentation of these factors in the context of the CSTG wave propagation hypothesis challenging. The predominant consideration which the hypothesis has clarified is the thermodynamic cause of the PMTP. Joseph and Schickele [26] alluded to some considerations responsible for varying levels of accuracy of thanatochronometry methods and this dissertation continues with that approach, in which implication of the hypothesis to present-day methods of thanatochronometry are discussed.

### 5.3.1 Relevance of Newton's Law of Cooling

Strictly speaking, Newton's Law of Cooling [6] only describes cooling that occurs on the surface of a body to the external environment. Even when describing surface cooling, the Law specifically describes cooling that occurs only by thermal convection and does not describe surface cooling by thermal conduction or by thermal radiation, which are governed by separate physical laws. In most post-mortem cooling scenarios a proportion of the total-body surface may be in contact with a solid surface, such as the ground, while the remaining proportion is freely exposed to air. Body posture largely determines these proportions. Newton's Law of Cooling applies only to the proportion of the body's total surface that cools by thermal convection, i.e. exposure to air or fluids. Newton's Law is therefore not valid to describe post-mortem cooling of the core of a body because by definition, the core is *always* surrounded by solid body mass and therefore loses heat exclusively by thermal conduction to the surface. Cooling of the core, or any internal part of the body, is governed exclusively by Fourier's Law of Cooling as mentioned earlier.



With the exception of Smart [60], virtually all earlier authors such as Rainy [5], Burman [7],Womack [8], Smith and Simpson [67], Marshall [17,18,19,20, 21,22,23, 24], Henssge and Henssge with others [1, 33, 34, 35, 36, 37, 38, 39, 40, 41, 42, 43, 44, 61, 68], Brown and Marshall [27] and many others, have always

referred to Newton's Law of cooling explicitly, or implicitly through applying methods derived by other authors who based their work on the Law, *even though core is where they had measured the temperature from*. Admittedly many of them did realise that Newton's Law was not valid due to the presence of PMTP on cooling curves. The inappropriate attribution of post-mortem core cooling to Newton's Law arises when core-cooling is regarded as being analogous to or representative of total-body cooling. The two entities are different. The reasons given by Brown and Marshall [27] of why Newton's Law was not valid for describing the PMTP did not mention the fact that the Law does not apply to the core of the body, and that it is specific only for skin heat loss by thermal convection. Body size as a consideration they gave is discussed in subsequent sections. Brown and Marshall's reasoning does not make the differentiation between surface cooling and core cooling.

The reasons given by Marshall and Hoare [22] of why Newton's Law was not valid for describing post-mortem cooling was of a constant $Z$ which represents thermal resistance between the body and the ambient temperature and caused the double-exponential shape of the time-temperature curve as opposed to a single-exponential shape of a Newtonian time-temperature curve. This consideration is also discussed in subsequent sections. They also did not mention the fact that the Law is only valid for describing surface cooling, and even then valid only for the proportion that cools by thermal convection.

The single exponential shape of a time-temperature curve derived from a cooling body cannot automatically be attributed to Newton's Law of Cooling without specification being made of which body part the temperature was measured from. For example the core-cooling curve of the TGM illustrated in Fig. 2 has a single exponential shape, but such a shape is not and should not be attributed to Newton's Law of Cooling for the simple reason that the body part in consideration is the core. The practically straight part of the core cooling curve in Fig. 1 has religiously been attributed to Newton's Law of Cooling. Such attribution is clearly erroneous. Application of Newton's Law of Cooling to explain post-mortem body cooling when using core temperature measurements can be expected to yield meagre results [30].

### 5.3.2 The Post-mortem Temperature Plateau

The author's own definition of the PMTP is: *'the time interval between heat withdrawal or death and the moment core temperature begins to decrease'*. The reason this distinction is made is that some authors [22, 44] include into the definition of PMTP that part of the time-temperature curve in which there cooling of the core does occur, albeit initially slow. The second reason is that other authors [57] have recently suggested that post-mortem temperature increase should be included into the definition of the PMTP. The author disagrees with both these definitions.

According to this definition the initially slow rate of core cooling that is usually observed before the steepest part of the curve is not part of the PMTP. In this dissertation the presence or absence of the post-mortem temperature plateau was experimentally and theoretically demonstrated to be dependent on the magnitude of temperature gradient between the surface and the core at the time of death. The wave model explains that the core-to-surface temperature gradient physically propagates from the surface to the core at the beginning of cooling when the initial surface and core temperatures are equal. The post-mortem temperature plateau is the result of a delay in this propagation. The length of the post-mortem temperature plateau is shown to be dependent on the depth of thermometry in relation to core and the surface. Absence or presence of the post-mortem temperature plateau, in

turn, affects the overall shape of the post-mortem temperature curve. The fact that these two considerations, i.e. magnitude of CSTG at death and depth of thermometry, and their consequences have not been taken into account in previous observations is thought to be a reason for the apparently unpredictable nature of the post-mortem temperature plateau. The hypothesis demonstrates that the core cools to the skin through the body, and that it is the skin that cools to the external environment. It also verifies how current thermometric thanatochronometry methods are compound methods that, in reality, describe the two cooling processes simultaneously.

### 5.3.3 Body Core

Current methods of thermometric thanatochronometry make use of core temperature because the core is obviously less prone to temperature fluctuations that readily affect skin temperature. Technically speaking, the core of any three dimensional body is the geometric centre of that body and can be defined as an infitesimal point furthest from any surface. However, for practical purposes any body's core is often regarded as an area of varying size and of uniform chosen characteristics, i.e. temperature, around this infitesimal point, so that making reference to any point within that uniform area would have no consequence. In regular and geometrically symmetrical shapes such as a sphere or a cylinder, the distance from this 'practical core' to the surface is naturally slightly less than the strict geometric radius, depending on the size of the 'practical core'.

According to the American Meteorological Society, the thermal core of a body is defined as the interior of a convective thermal that is relatively undiluted by lateral entrainment or intromission. An intrinsic characteristic of the thermal core is that its temperature is higher than of any other part of the body during the entire cooling interval so that the term 'hot spot' is appropriate to define it. The size of a body's thermal core is a function of the body's temperature distribution and when temperature is equal in every part of the body its size is equal to the radius of the body, i.e. the thermal core is anywhere in the body. Such as situation is

encountered in a cooling dummy whose core temperature is equal the ambient temperature of an incubator.

However, during post-mortem cooling the thermal core is not a static entity that is only defined by anatomical consideration, but it is dynamic as a result of the propagation of the CSTG wave. The diameter of this '*post-mortem thermal core*' gradually decreases radially away from the surface as a result of CSTG wave propagation during the PMTP. Thereafter the size of the thermal remains constant until the last part of the CSTG wave reaches it at the end of cooling, after which the thermal core completely disappears when the temperature in all parts of the body is identical. Incidentally, and perhaps paradoxically, the uniform temperature distribution that occurs at end of cooling defines a new post-mortem thermal core whose size is also equal to the body radius as before, should a new CSTG wave propagate as a result of further surface cooling.

The increase in the absolute error with increasing post-mortem interval that was observed by James and Knight [25] and Simonsen *et al* [28] is now thought to have been the consequence of decreasing size of the post-mortem thermal core. The exact location of the post-mortem thermal core at any time during cooling is determined by:

(i) the position of the geometric centre of the body,

(ii) thermal properties and spatial distribution of organs between the surface and the core,

(iii) temporal and spatial uniformity of surface cooling and, (iv) by the post-mortem interval itself as mentioned earlier.

In an isotropic body such as a cooling dummy, the centre of the post-mortem thermal core remains in the geometric centre at any time during cooling. This is because all CSTG waves from the entire body surface propagate at identical rates and therefore meet at the geometric core that is furthest from any surface, whose temperature remains higher than that of any other part of the body, thus defining the thermal core.

The post-mortem thermal core remains in the geometric centre of a body on two conditions:

(i) at any given time during post-mortem cooling the rate of surface cooling has to be identical on every part of the surface and,

(ii) the rate of surface cooling must remain constant for the duration of post-mortem cooling.

Failure to meet these two conditions results in the formation of new CSTG waves on the surface of the body. For example, intense but localised surface-cooling disproportionate to that occurring on the rest of the body surface results in the formation of a new CSTG wave whose amplitude is larger than that of other CSTG waves in adjacent body parts that are cooling less intensely. Such a disproportionate CSTG wave propagates and causes disproportionately higher rates of cooling in surrounding body parts compared to cooling rates elsewhere in the body. The result is that the location of the post-mortem thermal core shifts away from the intensely cooled areas to warmer parts of the body.

In an anisotropic body such as the human torso different solid organs have different thermal properties [70] and are distributed asymmetrically in the axial plane. The rate of CSTG wave propagation is slower in organs with high thermal resistivity so that those organs serve as thermal reservoirs that trap heat for longer periods. The relative spatial distribution of such organs in the torso influences the location of the post-mortem thermal core. The location of the post-mortem thermal core in the human trunk cannot be assumed to be at the geometric centre. The post-mortem thermal core is therefore a dynamic entity that is quite distinct from a non-specific 'body core' whose definition is identical to that of the ante-mortem core. To accept that the depth of the thermal core does not need to be quantified as long as it is beyond the immediate influence of external factors that affect skin

temperature, as described by Marshal and Hoare [22], would be poor judgement. Current methods of thermometric thanatochronometry need to take these considerations of the post-mortem thermal core into account.

### 5.3.4 Body Mass and Body Radius

The hypothesis suggests that a body with a bigger radius can be expected to have a longer PMTP and thus a longer total post-mortem interval than a body with a smaller radius. A larger radius in a *solid* body equates to increased body volume, increased body weight and increased surface area. The extent of increase of body weight relative to surface area depends on density of the body, so that weight increase is proportionately more in a denser body of the same volume and/or surface area, and vice versa. Increase in radius of the human body is largely due to adipose tissue and solid organ size whose density and thermal conductivity remain identical in different bodies. An increase in radius without an increase in density or in thermal resistivity of viscera therefore increases the body's heat storing capacity but also increases the surface area through which thermal conduction, thermal convection and thermal radiation occur.

The relationships between body mass, body radius and surface areas, represented by the body mass ratio $A/M$ by de Saram [12] and by the body-specific constant $Z$, explain the difference in cooling rates between lean and fat bodies that have been observed in many studies.

### 5.3.5 Temperature-depth to Body Radius Ratio

The hypothesis suggests that the ratio of temperature-depth relative to body radius affects the shape of the temperature-time curve by determining the presence or absence of the post-mortem temperature plateau. A cooling curve plotted from temperature measurements taken at or close to the thermal core will have a post-mortem temperature plateau, while a cooling curve plotted from temperature measurements taken simultaneously but close to or on the surface, will have a single exponential shape with no post-mortem temperature plateau. Cooling curves from incremental radial distances from the surface towards the thermal core progressively evolve in shape until a post-mortem temperature plateau appears. As an example, Fig. 6 shows a computer-generated illustration of time-temperature curves from a 50 litre polystyrene sphere using advance thermo-analytic software [69]. Although the illustration represents cooling of a sphere which is very similar to that of a cylinder, it demonstrates shape evolution of time-temperature curves with increasing radial distance from the surface to the core, as can be expected in a human body. The time-temperature curve with the longest plateau is that of the core of the sphere (green line).

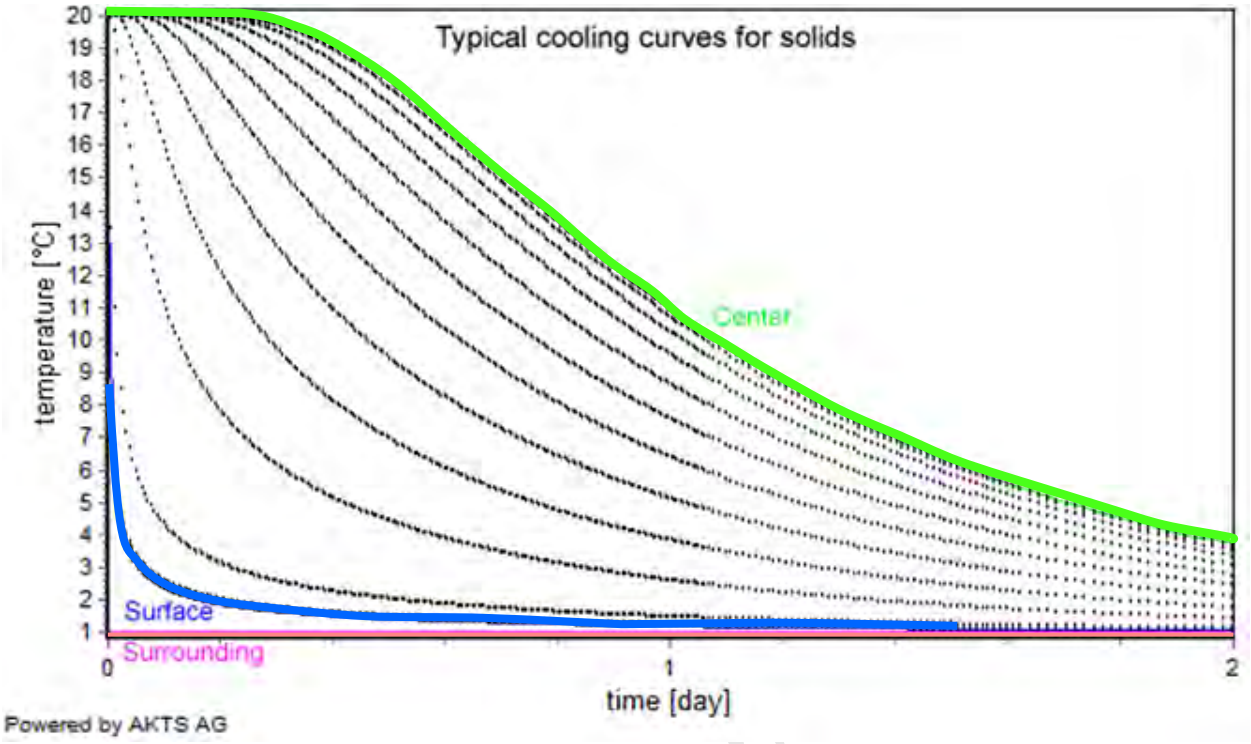


Fig. 5 illustrates computer-generated temperature-time curves of a 50 litre polystyrene sphere cooling from an initial temperature of 20°C in an ambient temperature of 1°C. The **green** line represents the core temperature curve, the **blue** line represents the surface temperature curve and the flat **pink** line represents the ambient temperature, © 2013, AKTS (http://www.akts.com/thermal-safety-overview.html) Used with permission from AKTS.

The notion by Sellier that the post-mortem temperature plateau can be explained by purely physical process and is not a phenomenon unique to biological bodies is also reiterated. The hypothesis suggests that as long as the ratio of temperature-depth to body radius is known:

(i) using body weight to calculate the post-mortem interval and subsequent calculation of the value of *B* as per the Nomogram method may not be necessary after all, and

(ii) thermometry can be at any depth so that all the considerations regarding the post-mortem thermal core discussed earlier, which should be considered by current methods, are not necessary to account for. Accurate quantification of body weight at the incident scene is logistically onerous, more likely estimations are done.

Regarding experimental work by previous authors, insertion of a thermometer to identical depths in human bodies irrespective of their axial radii can be expected to result in the thermometer tip being at non-identical depths relative to body radius: in some cases the thermometer tip may be at the thermal core and in other cases it may not be. To make an example, a thermometer inserted to a depth of 8cm from the surface of a body whose axial radius is 20cm will result in the thermometer tip being 12cm shy of the geometric core. However, insertion of a thermometer to the same depth of 8cm in a body whose axial radius is only 11cm will result in the thermometer tip being just 3cm shy of the geometric core. All else being equal, thermometers whose temperature curves show a post-mortem temperature plateau can be regarded as having been closer to or at the thermal core when compared to thermometers whose temperature curves do not show the post-mortem temperature plateau. In all studies using cooling dummies [35, 36, 37, 38, 40, 61, 62] axial depths of thermometers or relative to the radii of the cooling dummies were not

measured. With microwave thermography as used by Al-Alousi [45, 46, 47, 48, 49, 50, 51] it is not possible to determine the temperature-depth.

### 5.3.6 Route of Core Thermometry

Today the rectal route is the gold-standard method of core thermometry for thanatochronometry, wherein the thermometer is inserted to a depth of 3 to 4 inches into the anal sphincter, and its use dates back to 1868 by Rainy [5]. Liver thermometry is occasionally regarded as being more appropriate under certain circumstances. However there is no literature on the scientific justification for using rectal thermometry at those depths to represent post-mortem core temperature. Temperature-depth, as discussed earlier, is crucial as it affects the presence or absence of the PMTP by determining the propagation distance of the CSTG wave.

The rectum is known to be not at the centre of the torso [31] and post-mortem temperature distribution along the length of the rectum is not really known. The distance from the external anal sphincter to the core is rigid due to anatomical considerations and is independent of how fat or thin a body is; whereas a body's abdominal radius varies mainly due adipose tissue thickness. From personal experience with rectal thermometry the axis of the temperature probe is often at an angle of ~60° from the body's axial plane. The result is that the probe depth is more than the shortest possible radial distance from the surface that would be taken by the CSTG wave. Therefore it is difficult to determine the true axial temperature-depth with rectal thermometry. In addition, during rectal thermometry the buttocks have to be manually parted to visualise the sphincter and upon release they

automatically assume their natural apposition, sandwiching most of the temperature probe outside of the anal sphincter. It could be argued that the part of the probe between the buttocks is thermally 'inside the body' and that the depth of the probe tip from the skin of the buttocks to the core is potentially increased in comparison to the distance from anal sphincter to the core.

Temperature distribution in the body during life is known to vary according to the depth from the surface. The inner core in life has the highest temperature and the skin has the lowest temperature. Isotherms of the head and trunk in life [70] illustrate a temperature gradient with increasing depth from the surface to the core. Rectal temperatures in living humans vary with depth from the anus [71]. Although it is accepted that a temperature gradient exists between the surface and the core at any time during post-mortem cooling before the core temperature reaches the ambient temperature, there is no data of post-mortem temperature distribution with respect to inhomogeneity and geometry of the human body. To clarify these the author carried out a small study in which temperature measurements were made either from the anal sphincter into the rectum or from the skin into the liver at 10mm increments using a 10mm thick, 220mm long rigid K-type thermocouple probe.

As was to be expected, temperature values did increase with increasing depth towards the centre of the body. Values increased less predictably in the upper layers during liver thermometry, but changed abruptly on penetration of the liver capsule characterised by a sudden decrease in resistance to advancement of the thermocouple probe. In one body of 140mm radius the temperature continued to increase with each 10mm increment after capsular penetration until the probe was at a depth of 120mm from the skin, beyond which the temperature did not increase with further probe advances. The post-mortem thermal core of this body was thus up to 20mm from the geometric core in the axial direction, or it had a diameter of 40mm in the geometric core.

In this small study the average temperature distribution in rectal thermometry was found to be ~0.1°C per 10mm depth. In this route the post-mortem interval itself affected depth-temperature distribution: in the very early post-mortem period more of the deeper layers had identically high temperatures, with only the few outer layers having lower temperatures. In the later stages of post-mortem cooling virtually all depths had different temperature measurements. In other words the size of the post-mortem thermal core decreased with increasing port-mortem interval, as expected. In bodies where rectal thermometry was undertaken it was observed that the thermocouple probe rarely advanced beyond the 100mm depth into the anal sphincter, an observation that was thought to be due to the probe tip

reaching the sacrum. The consensus from this study was that the liver rather than the rectal route was more practical for determining temperature-depth. Insertion of a temperature probe at 90° to the abdominal skin at the radial plane decidedly ensures that probe depth is a true reflection of the radial temperature- depth. Differences in shapes of time-temperature curves between rectal and liver measurements, as observed by Marshall and Hoare [22], may have been due to differences in the true temperature-depth to body radius ratio between these two routes.

### 5.3.7 Skin Temperature

The hypothesis suggests that the core cools to the surface/skin, and it seems logical that during thanatochronometry core temperature must be correlated directly to surface temperature. The reasons that all modern methods of thanatochronometry do not measure skin temperature, but instead correlate core temperature directly with ambient temperature are multifaceted and have had a self-perpetuating effect on the field of thanatochronometry research and subsequent variations in success rates of such methods.

- The first reason may be that earlier researchers [5] realised that skin temperature was unreliable for thanatochronometry as it was easily influence by fluctuations in ambient temperature.
- The second reason may be that at the end of cooling, core temperature always reaches ambient temperature, an observation that can lead to the erroneous belief that the core cools directly to ambient air. As it is known, the core loses heat first to the skin through the body mass in-between: it is the skin that loses heat to the external environment. At any given time $t$ during post-mortem cooling the core temperature aspires to become whatever the surface temperature is at time $t$, notwithstanding the fact that the surface/skin itself at time $t$ aspires to become whatever the ambient temperature is at time $t$. Although it is known that the skin loses heat by

thermal conduction, thermal convection and thermal radiation, the emphasis of early and current thermometric thanatochronometry methods is predominantly on cooling by thermal convection, as demonstrated by application of ambient temperature in calculations, and to a less extent on thermal radiation and convection. For example the estimator for time-dependent skin temperature decrease rate by Mall *et al* [73] is based on Newton's Law of cooling, and therefore only addresses skin cooling by thermal convection. Cooling by thermal conduction and by thermal radiation has been largely ignored.

- The third reason may be that measuring the temperature of skin or clothes is not necessary as long as resistance of heat flow from the core through different barriers to the external environment was considered as a single entity whose magnitude can be derived by simple addition of the individual resistances of the different components.



The result was that the significance of considering surface temperature in understanding core cooling may have been lost in translation. In a number of studies that examined skin temperature [13 28, 72, 73] its relationship to core cooling as described by the CSTG wave propagation hypothesis could not be appreciated. The danger of not measuring surface temperature in experimental studies, especially when using recently-deceased human bodies received from

elsewhere, is that at the time of thermometry there may be a CSTG that is unbeknown to the observer, which would determine the presence/absence and length of the post-mortem temperature plateau and thus affect the shape of the entire cooling curve. The effect of a well-established CSTG present at the time thermometry, irrespective of the manner in which that CSTG was brought about and even if the core has not yet cooled from its initial temperature at death, is the same as though the CSTG had propagated from the surface of a body whose initial temperature distribution was uniform. Considerations raised by the hypothesis in previous sections make it apparent that although skin thermometry is not necessary, skin cooling as the primary method by which the body loses heat to the environment requires a more comprehensive understanding and consideration.

### 5.3.8 Standard Cooling Conditions

When one considers that a body cools by a combination of thermal conduction, thermal convection and thermal radiation it becomes apparent that 'Standard Cooling Conditions' are anything but standard because they omit other factors known to affect body cooling that also need to standardised, or at least quantified, so as to be compensated for during thanatochronometry.

(i) In nearly all cooling studies using human bodies by previous authors, conditions of cooling *prior to* 'standard cooling conditions' being instituted or thermometry being undertaken were not standardised, as though the skin would have not been cooling in that time. In such studies the circumstances of death before the bodies are collected for such studies are rarely mentioned. The types of surfaces on which bodies lay at or after death, but before 'standard cooling conditions' apply, are often referred to briefly and in passing and their thermal conductivity or temperature and the total contact-time are never measured. Body posture at death is never mentioned. Information about air temperature, air humidity, thermal radiation, wind speed and clothing *prior to* 'standard cooling conditions' / thermometry are often omitted and/or not standardised. All these factors are critical because they determine the rate of skin cooling immediately after death, which then determines magnitude of the initial part of CSTG wave

propagation (the peak). Immediately at death or on heat withdrawal the rate of surface cooling is extremely rapid and would form the amplitude of the CSTG wave which would propagate towards the core. The propagation rate and amplitude of that CSTG wave would therefore be outside the control of the observer by the time Standard Cooling Conditions take effect, at which time the peak of the wave would be somewhere between the surface and the core. As the hypothesis states that the steepest part of the temperature-time curve is due maximum rate of cooling as a result of the CSTG wave peak, and that the length of the post-mortem temperature plateau is determined by the body radius or the temperature-depth to body radius ratio, 'standard cooling conditions' have no effect on these first two parts, i.e. the post-mortem temperature plateau and the steepest part of the core temperature-time curve under such experimental conditions. What would determine presence or absence of the post-mortem temperature plateau in standard cooling conditions is the depth of thermometry in relation to the propagating peak of the CSTG wave (the temperature-depth to body-radius ratio). If the thermometer is inserted to deep parts of the body, the tip of the thermometer 'overtakes' the wave peak to end up in uncooled depths where the wave peak would not yet have arrived. The delay of the wave peak in 'catching up' with the thermometer tip

manifests itself as the post-mortem temperature plateau at that depth. If insertion of the thermometer is delayed until after the wave peak has reached the depth of thermometry, there would be no post-mortem temperature plateau because the body would have begun to cool at that depth. Pilot-broken studies, or studies under non-standard cooling conditions are merely a natural continuation of non-standard cooling conditions that would have existed before thermometry, and they predictably result in different skin cooling rates and subsequent changes in CSTG magnitudes.

(ii) As mentioned earlier, thermal properties of the surface on which post-mortem cooling occurs affect the position of the post-mortem thermal core by affecting surface temperature. In Standard Cooling Conditions bodies are often said to be placed on a 'thermally indifferent surface'. But what is a thermally indifferent surface? What is it that is indifferent about such a surface? Is it the temperature? And what is the indifference towards? Is it towards the body itself? In the author's opinion the term 'thermally indifferent surface' should be used to refer to indifference, or equality, of *thermal conductivity* and *temperature* of that surface on which a body cools by conduction, in relation to the *thermal conductivity* and *temperature* not of the body itself, but of *air* to which the rest of the body cools by convection. In the supine

position, the skin of a naked body that cools by thermal conduction is the proportion in which contact pallor is observed at autopsy. The interface temperature of the skin that is in contact with any surface is determined by the *thermal conductivity and temperature of both surfaces* and is directly calculated as follows:

$$T_s = \frac{\sqrt{(\lambda\rho c_p)_s}T_{s,i} + \sqrt{(\lambda\rho c_p)_o}T_{o,i}}{\sqrt{(\lambda\rho c_p)_s} + \sqrt{(\lambda\rho c_p)_o}} \quad (7)$$

where $T_{s,i}$ is the initial skin temperature, $T_{o,i}$ is the initial object temperature, $\lambda$ is the thermal conductivity, $\rho$ is the density and $c_p$ is the thermal heat capacitance. From equation (5) it is clear that the interface temperature is dominated by the temperature of the surface with the larger $\lambda\rho c_p$.

Thermal indifference of temperatures and thermal properties a surface ensures that the rate of surface cooling is uniform throughout the body, as though the entire surface were cooling in air exclusively by thermal convection. This consideration, in turn, ensures that the position of the post-mortem thermal core does not change, and is necessary because in most of the literature on post-mortem cooling, a proportion of the body's skin is always in contact with a solid surface (the ground, a metal plate, a wooden surface or other 'thermally indifferent surface'

not otherwise specified), while another proportion body is freely exposed to air. Thermal indifference of a surface cannot be with reference to the body itself – the implication would be that (a) such a surface has the same thermal conductivity as that of the skin and that, (b) such a surface would have been pre-heated to the same initial temperature as the skin. Of cause such considerations are never a reality.

Air at 25°C has thermal conductivity of 0.024 W/(m.K), Styrofoam = 0.033 W/(m.K), urethane foam = 0.021 W/(m.K) and cotton wool = 0.029 W/(m.K) [74]. Thermal conductivity of stainless-steel can be as high as 50 W/(m.K). Concrete has thermal conductivity of 1.13 W/(m.K) [75] and the thermal conductivity of wood varies according to the type of tree. Thus a statement about a 'thermally indifferent surface' that fails to demonstrate, at the least, that the thermal conductivity of such a surface is in fact equal to the thermal conductivity of the surrounding air is just meaningless. Many other considerations that are known to affect thermal conductivity of air, such as relative humidity and pressure, do not appear under the definition of 'Standard Cooling Conditions'.

# CHAPTER SIX

## DISCUSSION: The CSTG Wave Propagation Hypothesis and Methods of Thanatochronometry

Fourier's Law describes unsteady-state heat transfer of the body by conduction. It is applied in engineering sciences, thermodynamics, build and thermal comfort sciences to solve complex heat transfer conditions. Such application takes into account many of the considerations already addressed. A few authors [15, 16, 27, 60] have attempted thanatochronometry by application of this Law in its various expressions, but without the considerations that are raised by the core-surface temperature gradient wave propagation hypothesis. In order to place the hypothesis into perspective, the following sections discuss all abdomino-pelvic thermometric thanatochronometry.

## 6.1 Fourier's Law and methods based on it

From equation (5), the basic Fourier equation for one-dimension heat transfer in a cylinder of infinite length with radius $r$ is:

$$\frac{\partial T}{\partial t} = \alpha\left(\frac{\partial^2 T}{\partial r^2} + \frac{1}{r}\frac{\partial T}{\partial r}\right) \tag{8}$$

where $\partial T =$ temperature difference of the body from time $t_0$ to time $t$; $\partial t =$ time difference from time $t_0$ to time $t$; and $r$ = any radial point. The term $\alpha$ represents thermal diffusivity $\frac{\lambda}{\rho\, c_p}$. The analytical solution to one-dimensional transient heat conduction in a cylinder of radius $r_0$, subjected to convection on all surfaces and subjected to constant ambient temperature, can be expressed in terms of an infinite series of cosine functions and implicit equations [76] as:

$$\theta = \sum_{n-1}^{\infty} \frac{2}{\lambda_n} \frac{J_1(\lambda_n)}{J_0^2(\lambda_n) + J_1^2(\lambda_n)}\, e^{-\lambda_n^2 \tau}\, J_0(\lambda_n r/r_0) \tag{9}$$

where $\theta = [T(\mathrm{r},\mathrm{t}) - T_i]/[T_\infty - T_i]$ and is the dimensionless temperature in which $T(\mathrm{r},\mathrm{t})$ is the temperature at time $t$ and at some radial position $r$ between the surface and centre; $T_i =$ initial uniform temperature of the body; $T_\infty =$ eventual uniform temperature at the end of cooling; $\lambda_n$ is the $B_i$ (Biot number) = root of $\lambda_n \frac{J_1(\lambda_n)}{J_0(\lambda_n)} = hr_0/\lambda$, whose values are listed in Annexure B (Table 4); $\tau = \alpha t/r_0^2 =$ $F_o$(Fourier number); and $J_0$ and $J_1$ are zeroth- and first-order Bessel functions of

the first kind respectively, whose values are given in Annexure A (Table 3). This Fourier series solution equation should be applied only to cooling conditions in which surface cooling occurs by thermal convection. Such a condition of use is testament to considerations regarding a 'thermally neutral surface' that were discussed earlier. The second condition of its use is that the ambient temperature should remain constant during the cooling interval. The reason for this condition is to eliminate the effect of secondary or subsequent CSTG wave peaks that would form with changes in the skin cooling rate, which would disturb temperature distribution between the surface and the core.

The Fourier's series of expansions adequately not only mathematically expresses the sigmoid nature of the post-mortem cooling curve, but also explains it. There are several noteworthy points about the Fourier's series of expansion represented by equation (7) in relation to the CSTG hypothesis:

i. the value of $\lambda$ in the Biot number represents internal thermal conductivity of the body between the surface and the core, which affects the CSTG wave propagation rate according to the hypothesis,
ii. the value of $h$ in the Biot number represents convective heat transfer coefficient on the surface, which determines the rate of surface cooling, which in turn determines the formation of the CSTG wave, especially its peak,

iii. the Fourier number $\tau$ is a function of the body's thermal diffusivity $\alpha$, which determines the rate of CSTG wave propagation. Thermal diffusivity is a function of body density $\rho$, body's thermal heat capacitance $c_p$ and body's thermal conductivity $\lambda$,

iv. the temperature-depth to body radius ratio $r/r_0$ determines the presence/absence and length of the post-mortem temperature plateau, and

v. that it can be expressed in many forms depending on the circumstances of cooling known as *initial conditions* and *boundary*/*end conditions*.

*Initial Conditions*

There are only two initial conditions that apply to any cooling process: when the initial temperature distribution of the body is uniform throughout and when it is not uniform. The choice of expression of Fourier's Law that needs to be applied for a particular cooling circumstance has been a source of variation in all the four studies in which this method was applied. If there is a temperature distribution at the beginning of cooling that is a function of radius *r,* such as the CSTG of ~3 to 4°C known to exist in life and therefore at the time of death in most instances, the form of equation (7) that expresses temperature distribution after time *t* is given as:

$$T_a = T(\mathrm{r},\mathrm{t}) - \sum_{i=1}^{n} A'_n J_0(\lambda_n \cdot r/r_0) e^{-[\lambda_n^2 \theta]} \cdot \int_0^r r\, f(r) J_0(\lambda_n \cdot r/r_0) dr \qquad (10)$$

where $A_n' = 2/[r_0^2 J_1(\lambda_n)]$ and is a function of the Biot number whose values are listed in Table 4. Equation (8) illustrates the relationship between $T$(r, t), which is the temperature measured at a known radius $r$ at time $t$, with the ambient temperature $T_a$. This is the equation that may be applied and reapplied every time the ambient temperature $T_a$ changes during the course of cooling, during which there would be a known radial temperature distribution, thus negating the requirement for a constant ambient temperature.

*Boundary/end conditions*

A boundary condition refers to the uniform temperature that a body under consideration will reach at the end of heat transfer. A boundary condition is defined by the temperature difference between a body and its immediate surroundings before cooling commences. Such a temperature difference determines the direction of heat flux. The context of heat transfer needs to be clearly defined so that the correct boundary condition is applied into the Fourier equation. In the context of total-body cooling (core and surface) the boundary condition is admittedly the ambient temperature. However when core cooling is in consideration, the hypothesis suggest that the boundary condition must be surface temperature $T_s$ rather than ambient temperature $T_a$. Regarding the consideration of substituting $T_\infty$ by $T_s$ in calculating the value of the dimensionless temperature $\theta$, the Fourier method adds the value of the surface convective heat transfer

coefficient $h$ to the value of internal thermal resistivity that exists between the surface and the core to get a single value represented by the Biot number $\lambda_n$, so that $T_a$ can represent $T_\infty$ as suggested by Joseph and Schikele [26]. The need for the onerous task of measuring total-body skin temperature is thus eliminated.

Suspension of the wooden cylinder by Smart [60] allowed for all the surface of the cylinder to cool in air by thermal convection and thermal radiation, circumventing the problem of a "thermally indifferent surface" as discussed in the previous sections. Despite the deliberate choice of a wooden cylinder, whose thermal diffusivity is equal to that of a human trunk, which is accepted to cool as a cylinder of infinite length, the radius $r$ was not used to derive the value of the Fourier number $F_o$. The reason given was that the wooden cylinder did not have an infinite length as its length/diameter ratio was 2. This logic seems self-contradictory, especially when values of both $\alpha$ and $r_0$ were known to him.

The terms in the series solution in equation (9) converge rapidly with increasing time, so that keeping the first term and neglecting all other terms, if the value of the Fourier number $\tau > 0.2$, results in an error margin of less than 2%. When all the other terms are neglected equation (7) can be expressed as a **one-time approximation** of the core temperature at the centre of the cylinder where $r = 0$ in the form:

$$\theta_0 = \sum_{i=1}^{n} A_1 e^{-\lambda_i^2 \tau} \quad (11)$$

where $A_n' = 2/[r_0^2 J_1(\lambda_n)]$ and is a function of the Biot number and its values are listed in Table 4. This approach was applied by Sellier [16], Fiddes and Patten [15] and by Brown and Marshall [27]. However, such an approach automatically implies that the temperature was measured exactly at the core of the body, which itself implies that the radius of the body $r_0$ was known so that temperature-depth was consciously made equal to body radius, i. e. $r$ is equal to zero. It also implies that the value of the Fourier number $\tau$ was confirmed to be > 0.2. Apart from the 2% error margin, application of equation (9) without these considerations is clearly problematic and will produce variation. The same consideration is true when this method is applied on temperature measurements from other authors or previous studies, in which the value of $r$ is not equal to zero.

## 6.2 Internal Body-temperature-only (Time Dependant Z-equation) Methods

Regarding equation (4) that is the basis of these methods, Green and Wright [54] did not specify which part of the body the temperature $T$ was in reference to between the surface and the core. This differentiation is important, as discussed under the relevance of Newton's Law of Cooling. It is presumed that they referred to core temperature $T_c$, which is the furthest part of the body from any surface from which heat is lost. When equation (4) is compared to equation (6) that is the expression of the CSTG wave, it becomes apparent that the two equations represent the same concept. If indeed equation (4) makes a direct correlation between core temperature $T_c$ and ambient temperature $T_a$, it becomes apparent that the constant $Z$ represents a combination of internal body resistance $R_\theta$, which is between the core and the surface and is a function of the Fourier number, with the surface convective heat transfer coefficient $h$, which is a function the Biot number. The proponents of this method themselves describe the constant $Z$ as being 'the factor that determines how fast the temperature will fall in given circumstances'. The Nomogram method clearly also falls under this category, as it also features the constant $Z$, as discussed earlier.

What is noteworthy about equation (4) is that it can either represent Newton's Law or Fourier Law, depending on the entities between which heat transfer occurs: if heat transfer is between the core and the surface by thermal conduction, equation (4) represents the Fourier equation. But if heat transfer is between the surface and environment it represents the classical Newton equation. Confusion may arise when equation (4) is used to correlate core temperature directly to ambient temperature, in which case the two Laws comingle and make the context of the constant $Z$ less easy to define, hence the need to use the analytical solution in the form of equation (9). Internal-body-only thermometric thanatochronometry methods therefore intrinsically measure the skin's convective heat transfer coefficient $h$, which itself is an indirectly way of measuring skin temperature. They are therefore not truly internal-body-only methods, although superficially they appear to be. Hesnsge's Nomogram method (discussed later) also incorporates the cooling constant $Z$ in the exponential term of both terms.

The gradient between any two time points on a temperature-time curve, which is what these methods measure, represents the rate of temperature change that is equal to the inverse of the CSTG multiplied by thermal conduction of the body, according to the Fourier equation (6). Fig. 6 illustrates the relationship between the CSTG curve from Experiment 26 and the negative-gradient curve of the core-temperature curve.

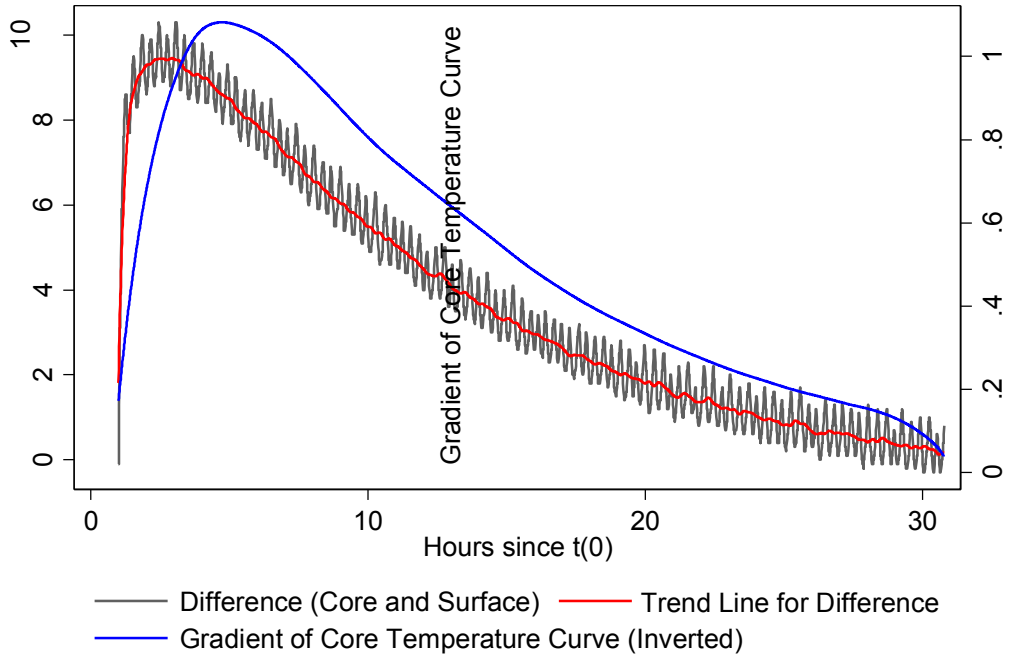


Fig 6. The CSTG curve in red is superimposed on the inverted-gradient curve of the core temperature curve in blue.

Although not a perfect match, the similarity of the two curves in shape and symmetry is obvious: the absolute difference is due to thermal resistance according to the Fourier equation (6). These Internal-body-only methods can be regarded as an indirect way of measuring the CSTG, i.e. skin temperature if the internal thermal resistance is known, and vice versa. The percentage method by Fiddes and Patten [77] is based exclusively on the Fourier series of solutions already discussed.

## 6.3 Marshall and Hoare's Cooling Formula

It is now apparent from the Cooling Formula in equation (1) that the second exponential term, which has the constant $A$ as an exponent and describes the PMTP, represents in reality a combination of all the factors that determine the length of the post-mortem temperature plateau as discussed in previous sections. Revisiting the Fourier equation (11), which is the **one-time approximation** method for $r = 0$ that was mentioned earlier that is an expression of:

$$\theta_0 = A_1 e^{-\lambda_1^2 \tau} + A_2 e^{-\lambda_2^2 \tau} + A_3 e^{-\lambda_3^3 \tau} + \cdots \qquad (12)$$

that has $n$ number of term, it is clear that the Cooling Formula is in fact the same as this method, but in which the number of terms is limited to just two. The value of the constant $A$ of the Cooling Formula therefore represents $A_1 = 2/[r_0^2 J_1(\lambda_n)]$, a function of the Biot number whose values are listed in Table 2. Likewise, it is clear that the value of the first exponent of the Cooling Formula that contains the cooling constant $B$ is a function of both the Fourier number $\tau$ and the Biot number $\lambda_n$, the latter whose values are listed in Table 4. In the Cooling Formula the independent variable time $t$ is part of the exponential term for both terms, and in the Fourier one-time approximation method the independent variable time $t$ is also part of the exponential term in the form of the Fourier number $\tau$. As mentioned before, application of the one-time approximation method requires the Fourier number $\tau$ to be > 0.2 and the temperature-depth to be equal to the body radius

(centre). To not satisfy these conditions is clearly problematic, the 2% error margin aside.

## 6.4 Henssge's Nomogram Method

The correlation between the cooling coefficient $B$ of the Cooling Formula with body mass $M$ is not surprising when one considers that the value of the surface convective heat transfer coefficient $h$ in the Biot number is equal to body volume divided by surface area $(V/A)$; having discussed the relationship of body volume and surface area to body weight of a solid object in earlier sections. Again one can appreciate that the Nomogram equation (2) is the same as the **one-time approximation** of the Fourier series of solutions equation (12), but in which the number of terms is limited to two in the same manner that the Cooling Formula is.

Reference to Table 4 infers that, for the value of the empirically determined cooling constant $A$ to be equal to 1.25, the Biot number of 'Standard Cooling Conditions' is in reality somewhere between 1.0 and 2.0. Because the second term in the Nomogram equation is $(1 - A)$, it is easy to appreciate the minus sign in front of it. In the context of the Fourier method, into which we have demonstrated that the Nomogram method falls, it is now apparent that the effect of variables for which Henssge empirically derived cooling factors is to either retard or accelerate the rate of skin cooling, which itself changes the value of surface convective heat transfer coefficient $h$ in the Biot number in both terms of the Nomogram equation.

Strong thermal radiation is one of five exclusion criteria for the application of the Nomogram method. Thermal radiation onto the body surface changes the surface convective heat transfer coefficient $h$ as well, so that measured values of thermal radiation near a body can be applied in thanatochronometry. The effect of a truly 'thermally neutral surface' is to make the convective heat transfer coefficient $h$ in the Biot number that is used to describe the proportion of skin cooling by thermal convection in air to be equal to the value of thermal conductivity $\lambda$ of that 'thermally neutral surface' that is used to describe cooling of the proportion of skin in contact with such as solid surface in equation (7). The effect of this consideration is to make the entire surface to cool as though exclusively by thermal convection – a prerequisite for application of the Fourier series solution.

### 6.4.1 Clothing and the Nomogram Method

When the Nomogram method is expressed as the Fourier one-time approximation method it is apparent that the effect of clothing can be alternatively factored by application of *clo* units to determine the value of surface heat transfer coefficient $h$ in the Biot number. *Clo* units express insulation by clothing, whereupon 1 *clo* = 0.155 K·m$^2$/W, a measure of thermal resistance. One *clo* is defined as *the amount of clothing insulation that allows a living person at rest to maintain thermal equilibrium in an environment at 21ºC in a normally ventilated room with 0.1m/s air movement. Above this temperature the person so dressed will sweat, whereas*

*below this temperature the person will feel cold*. According to the American Society of Heating, Refrigeration and Air-conditioning Engineers (ASHRAE) 55-2010's Standards [78], there are three methods for estimating clothing insulation using tables of measured *clo* values for various clothing ensembles in instances where the thermal resistance cannot be directly measured:

- If the ensemble in question matches reasonably well with one on Table 5 the indicated value of intrinsic clothing insulation can be used;
- It is acceptable to add or subtract garments on Table 6 from the ensembles in Table 5 to estimate the insulation of ensembles that differ in garment composition;
- It is possible to define a complete clothing ensemble as a combination of individual garments using Table 6.

The total value of *clo* for a given body can be arithmetically determined and added to the calculated value of the surface heat transfer coefficient.



### 6.4.2 Wind Speed, Air Humidity and the Nomogram method

For consideration of the effect of wind by the Nomogram method from the perspective of the one-time approximation equation, the convective heat transfer coefficient $h$ in the Biot number can be correlated with physical circumstances of heat transfer and physical properties and air flow conditions using empiric correlations that are usually in terms of four dimensionless numbers: Reynolds

($Re$), Nusselt ($Nu$), Prandtl ($Pr$) and Grashof ($Gr$) numbers. Other dimensionless numbers can also be used under specific cooling conditions.

For example, the Reynolds number is used for air flow characterisation and is expressed as:

$$Re = \frac{\mathrm{v}L}{v} \tag{13}$$

where v = mean velocity of the air relative to the cooling surface ($ms^{-1}$), $L$ = travelled length of the air over the cooling surface ($m$) and $v$ = kinematic viscosity ($m^2s^{-1}$) of air which is calculated as:

$$v = \frac{\mu}{\rho} \tag{14}$$

where $\mu$ = flowing air's specific viscosity and $\rho$ = air density, which itself depends on air temperature, relative air humidity and altitude above sea level. Air specific viscosity is a temperature-dependent variable. Application of this mathematically rigorous approach would allow for the effect of measured wind speed, relative humidity, and altitude above sea level which, together with *clo* untis can be used to calculate the rate of skin cooling by determining the value of the convective heat transfer coefficient $h$ in the Biot number. In this way the original aims of this study to empirically derive corrective factors for wind speed and air humidity become obsolete.

When the Nomogram method is viewed from the perspective of the Fourier method, it becomes apparent that it can be applied to *any* cooling condition, including 'unusual cooling conditions without any experience of a corrective factor' that Henssge conceded are another exclusion criterion for the application of the Nomogram method. The dependence of corrective factors on body weight under stronger thermic insulation conditions [40] is therefore a function of the Biot number. It can be predicted that if corrective factors for all the other variables that also affect the Biot number were to be devised, they would also show dependence on body weight, especially in their extremes. Given the diversity of all the considerations about thermometry and the Nomogram method, variations in the success rate in its field application [39] are understandable. The direct inclusion of body mass in the Nomogram method has resulted in the description of further formulae that relate errors of the calculated post-mortem interval as a function of the relative error of body mass[79]. The description of such compensatory methods is potentially perpetual.

## 6.5 Triple-Exponential Formulae (TEF) Method

When the Triple-Exponential equation (3) is compared to the Fourier **one-time approximation** method in equation (12), it becomes clear that the TEF equation is in fact the same as this method, but in which the number of terms $n$ is 3. The reason that those intercept-parameters $P_1$, $P_3$ and $P_5$ did not vary from case to case is now clear: they are a function of the same Bessel function of the zeroth order $A_1$ listed in Table 3. The reason exponent-parameters $P_2$, $P_4$ and $P_6$ varied from case to case is that they represent the Biot number $\lambda_n$, whose values are listed in Table 2 and which vary according to the root of the Bessle function $\lambda_n \frac{J_1(\lambda_n)}{J_0(\lambda_n)}$. Concerns about application of the one-time approximation method without measuring the values of $r_0$ and $r$ have already been addressed and in the TEF method are compounded by the use of microwave thermography in which the value of temperature-depth $r$ is unknown to begin with.

## 6.6 Heat-flow Finite Element Model

Although heat loss from the skin of the Heat-flow Finite-element Model occurred by a combination of thermal conduction, thermal convection and thermal radiation, thermal properties and temperature of the surface on which the model cooled were not mentioned. It is difficult to appreciate how the study evaluated the impact of heat loss by thermal conduction with the 'ground'. This may be attributed to the following of traditional practice of using the unqualified term of 'thermally neutral surface' when describing cooling in 'standard conditions'. Skin temperature was not measured on the model so the value of the CSTG at the beginning of cooling, i.e. initial conditions, could not be determined. Results of the post-mortem interval from the application of this model were compared with those derived from the Cooling Formula.

The Heat-flow Finite-element Model is attractive because it has nearly unlimited potential in simulating cooling conditions as realistically as can be achieved. It's only limitations are (i) understanding of the cooling process by the programmer, which affects the number of variables to be simulated for and the manner in which the effect of those variables is interpreted, and (ii) the computer's data handling capacity. For instance the Heat-flow Finite-element Model can be used to define the location of the post-mortem thermal core during cooling. In the discretization process the number of elements can be increased or the cube nodes could be substituted for prisms to form a Heat-flow Finite-element Model with realistic

curvilinear surfaces characteristic of the external human body and internal organ morphology, instead of the square Lego®-brick-like cube nodes. The Heat-flow Finite-element Model could easily be able to demonstrate the CSTG wave propagation and formation of the post-mortem temperature plateau and has the potential to demonstrate the relationship between core-to-skin cooling and skin-to-ambient cooling when the focus is on skin temperature.

## 6.7 Computer-based Methods

The computer method applied by K. Hiraiwa *et al* [31, 32] was based on equation (6), the basic Fourier equation for one-dimension heat transfer in a cylinder of infinite length, but in which the mathematical approach that they applied to its solution was not the infinite series solution method by Carslow and Jaeger [76], but was the finite-difference method for solving differential equations by Smith [80], due to the consideration that the ambient air temperature is not constant during cooling . Essentially the assumption made by this computer method is similar to that made by the one-time approximation method of the Fourier method, in the temperature measurement is of the geometric core where the value of radius $r$ is zero.

The authors using this method applied temperature measurements from de Saram [12] which had no measured values of body radius $r_0$ or values of 'rectal' temperature-depth $r$ (for which they assumed their subjects must have had similar torso radii to de Saram's) and in which the radial temperature distribution at the time of thermometry was unknown (for which they assumed it to have been zero). Their simulation failed to demonstrate the relationship between the post-mortem temperature plateau and the cylinder radius $r_0$, as suggested by the hypothesis. The effect of cylinder radius was to lengthen the time-temperature curve following the

post-mortem temperature plateau. The authors also cited difficultly in determining the heat transfer coefficient $h$ in the Biot number.

Another computer-based method [81] is a simple computer program modelled directly on Henssge's Nomogram method and utilises all the cooling coefficients and corrective factors already discussed.

# CHAPTER SEVEN

# CONCLUSION

This study failed in its primary objectives of empirically deriving corrective factors for air humidity and wind speed to be used in the Nomogram method. What it did do, ultimately, is to theoretically demonstrate how measured levels of air relative humidity and measured wind speed can be incorporated into formulae for thanatochronometry, not just for the Nomogram method. In the grander scheme, this study carries the first documented description of the Core-surface Temperature Gradient Wave Propagation hypothesis which describes total-body cooling. In this study the post-mortem temperature plateau could be made at will to either be present or absent, and factors that determine its presence/absence and length are:

(i) The rate of skin cooling that is governed by the surface convective heat transfer coefficient $h$ and determines the formation of the CSTG wave,

(ii) Body radius $r$ that determines the distance to be travelled by the CSTG wave from the surface to the core,

(iii) The body's thermal resistance that determines the rate of propagation of the CSTG wave from the surface to the core,

(iv) Thermometer-depth and thermometry route that define the temperature-depth to body-radius ratio $r/r_0$ that defines the distance travelled by the CSTG from the surface to the thermometer relative to the body radius,

(v) The magnitude and distribution of the radial temperature gradient (CSTG) at death / beginning of cooling / heat withdrawal (initial condition), and

(vi) Delays in thermometry after death / beginning of cooling / heat withdrawal that result in the establishment of a CSTG that is present at the time of thermometry.

An understanding of the core-surface temperature gradient wave propagation as a cause of the PMTP through the hypothesis presented in this paper enables better understanding of the process of total-body post-mortem cooling that challenges many norms and traditions that have become standard practice in the science of thermometric thanatochronometry:

(i) Newton's Law of cooling is relevant only to describe convective surface cooling and is not applicable when describing core cooling, for which Fourier's Law should be applied,

(ii) Body size factor affects a body's surface convective heat transfer coefficient $h$,

(iii) The post-mortem thermal core is a dynamic entity that is distinct from its physiological or ante-mortem counterpart,

(iv) All factors that affect the rate of skin cooling modify the value of the body's surface convective heat transfer coefficient $h$.

(v) The Fourier series of solution method describe post-mortem cooling adequately and is suitable for of thanatochronometry. Its flexibility allows for many considerations that affect CSTG wave propagation to be accounted for.

(vi) The Cooling Formula, Nomogram method and the Triple Exponential Formula method are a form of the **one-time approximation method** of the Fourier series solution for the centre of a cylinder of infinite length where $r = 0$. As such their success is limited if the radius is not measured to ensure that indeed $r = 0$. Their applicability can be expanded to any cooling condition in which the value of the surface convective heat transfer coefficient $h$ can be measured.

(vii) The route of core-thermometry needs to be standardised so that temperature-depth can be measured accurately. The hepatic route appears to be convenient for this purpose.

(viii) The thermal conductivity and temperature of any surface in contact with the body during post-mortem cooling need to be established when estimating the time of death.

(ix) Effects of thermal radiation need to be considered when estimating the time of death, especially in tropical and subtropical climates during summer months where thermal radiation from the sun may be significant.

Aims of future research will be to estimate time of death using measured values of wind speed, thermal radiation, air humidity, *clo* units and thermal conductivity of surfaces using the climate-controlled laboratory.

# ANNEXURE A

Table 3

The zeroth- and first-order Bessel Functions of the first kind

| $\eta$ | $J_0(\eta)$ | $J_1(\eta)$ |
|---|---|---|
| 0.0 | 1.0000 | 0.0000 |
| 0.1 | 0.9975 | 0.0499 |
| 0.2 | 0.9900 | 0.0995 |
| 0.3 | 0.9776 | 0.1483 |
| 0.4 | 0.9604 | 0.1960 |
| 0.5 | 0.9385 | 0.2423 |
| 0.6 | 0.9120 | 0.2867 |
| 0.7 | 0.8812 | 0.3290 |
| 0.8 | 0.8463 | 0.3688 |
| 0.9 | 0.8075 | 0.4059 |
| 1.0 | 0.7652 | 0.4400 |
| 1.1 | 0.7196 | 0.4709 |
| 1.2 | 0.6711 | 0.4983 |
| 1.3 | 0.6201 | 0.5220 |
| 1.4 | 0.5669 | 0.5419 |
| 1.5 | 0.5118 | 0.5579 |
| 1.6 | 0.4554 | 0.5699 |
| 1.7 | 0.3980 | 0.5778 |
| 1.8 | 0.3400 | 0.5815 |
| 1.9 | 0.2818 | 0.5812 |
| 2.0 | 0.2239 | 0.5767 |
| 2.1 | 0.1666 | 0.5683 |
| 2.2 | 0.1104 | 0.5560 |
| 2.3 | 0.0555 | 0.5399 |
| 2.4 | 0.0025 | 0.5202 |
| 2.6 | -0.0968 | -0.4708 |
| 2.8 | -0.1850 | -0.4097 |
| 3.0 | -0.2601 | -0.3391 |
| 3.2 | -0.3202 | -0.2613 |

# ANNEXURE B

Table 4

Coefficients used in the one-term approximate solution of transient one-dimensional heat conduction in cylinders (Bi = $hr_o/\lambda$ for a cylinder of radius $r_o$).

| Bi | $\lambda_1$ | $A_1$ |
|---|---|---|
| 0.01 | 0.1412 | 1.0025 |
| 0.02 | 0.1995 | 1.0050 |
| 0.04 | 0.2814 | 1.0099 |
| 0.06 | 0.3438 | 1.0148 |
| 0.08 | 0.3960 | 1.0197 |
| 0.1 | 0.4417 | 1.0246 |
| 0.2 | 0.6170 | 1.0483 |
| 0.3 | 0.7465 | 1.0712 |
| 0.4 | 0.8516 | 1.0931 |
| 0.5 | 0.9408 | 1.1143 |
| 0.6 | 1.0184 | 1.1345 |
| 0.7 | 1.0873 | 1.1539 |
| 0.8 | 1.1490 | 1.1724 |
| 0.9 | 1.2048 | 1.1902 |
| 1.0 | 1.2558 | 1.2071 |
| 2.0 | 1.5995 | 1.3384 |
| 3.0 | 1.7887 | 1.4191 |
| 4.0 | 1.9081 | 1.4698 |
| 5.0 | 1.9898 | 1.5029 |
| 6.0 | 2.0490 | 1.5253 |
| 7.0 | 2.0937 | 1.5411 |
| 8.0 | 2.1286 | 1.5526 |
| 9.0 | 2.1566 | 1.5611 |
| 10.0 | 2.1795 | 1.5677 |
| 20.0 | 2.2880 | 1.5919 |
| 30.0 | 2.3261 | 1.5973 |
| 40.0 | 2.3455 | 1.5992 |
| 50.0 | 2.3572 | 1.6002 |
| 100.0 | 2.3809 | 1.6015 |
| ∞ | 2.4048 | 1.6021 |

# ANNEXURE C

Table 5

Description of garment ensembles to be used for calculating clo[1]

| Ensemble Description | Clo |
|---|---|
| Walking shorts, short-sleeved shirt | **0.36** |
| Trousers, short-sleeve short | **0.57** |
| Trousers, long-sleeve shirt | **0.61** |
| Same as above, plus suite jacket | **0.96** |
| Same as above, plus vest and T-shirt | **0.96** |
| Trousers, long-sleeved shirt, long sleeve sweater, T-shirt | **1.01** |
| Same as above, plus jacket and long underwear bottoms | **1.30** |
| Sweat pants, sweat shirt | **0.74** |
| Long-sleeve pyjama top, long pyjama trousers, short ¾ sleeved robe, slippers (no socks) | **0.96** |
| Knee-length skirt, short-sleeved shirt, panty hose, sandals | **0.54** |
| Knee-length skirt, long-sleeved shirt, full slip, panty hose | **0.67** |
| Knee-length skirt, long-sleeved shirt, half-slip, panty hose, long sleeved sweater | **1.10** |
| Knee-length skirt, long-sleeved shirt, half-slip, panty hose, suit jacket | **1.04** |
| Ankle-length skirt, long-sleeve shirt, suite jacket, panty hose | **1.10** |
| Long-sleeve coveralls, T-shirt | **0.72** |
| Overalls, long-sleeved shirt, T-shirt | **0.89** |
| Insulated coveralls, long sleeve thermal underwear, long underwear bottoms | **1.37** |



[1] © 2013, ASHRAE (www.ashrae.org). Used with permission from ASHRAE.

# ANNEXURE D

Table 6

Clo values for different garments[2]

| Garment Description | clo | Garment Description | Clo |
|---|---|---|---|
| **Underwear** | | **Dress and Skirt** | |
| Bra | **0.01** | Skirt (thin) | **0.14** |
| Panties | **0.03** | Skirt (thick) | **0.23** |
| Men's briefs | **0.04** | Sleeveless, scoop neck (thin) | **0.23** |
| T-shirt | **0.08** | Sleeveless, scoop neck (thick), e.g. jumper | **0.27** |
| Half-slip | **0.14** | Short-sleeved shirtdress (thin) | **0.29** |
| Long underwear bottoms | **0.15** | Long-sleeve shirtdress (thin) | **0.33** |
| Full slip | **0.16** | Long-sleeve shirtdress (thick) | **0.47** |
| Long underwear top | **0.20** | | |
| **Footwear** | | **Sweaters** | |
| Ankle-length athletic socks | **0.02** | Sleeveless vest (thin) | **0.13** |
| Pantyhose/stockings | **0.02** | Sleeveless vest (thick) | **0.22** |
| Sandals/thongs | **0.02** | Long-sleeve (thin) | **0.25** |
| Shoes | **0.02** | Long-sleeve (thick) | **0.36** |
| Slippers (quilted, pile lined) | **0.03** | | |
| Calf-length socks | **0.03** | **Suit Jackets and Vests (lined)** | |
| Knee socks (thick) | **0.06** | Sleeveless vest (thin) | **0.10** |
| Boots | **0.10** | Sleeveless vest (thick) | **0.17** |
| **Shirts and Blouses** | | Single-breasted (thin) | **0.36** |
| Sleeveless/scoop-neck blouse | **0.12** | Single-breasted (thick) | **0.44** |
| Short-sleeve knit sport shirt | **0.17** | Double-breast (thin) | **0.42** |
| Short-sleeve dress shirt | **0.19** | Double-breast (thick) | **0.48** |
| Long-sleeve dress short | **0.25** | | |
| Long-sleeve flannel shirt | **0.34** | | |
| **Trousers and Coveralls** | | **Sleepwear and Robes** | |
| Short shorts | **0.06** | Sleeveless short gown | **0.18** |
| Walking shorts | **0.08** | Sleeveless long gown | **0.20** |
| Straight trousers (thin) | **0.15** | Short-sleeve hospital gown | **0.31** |
| Straight trousers (thick) | **0.24** | Short-sleeve short robe (thin) | **0.34** |
| Sweatpants | **0.28** | Short-sleeve pyjama (thin) | **0.42** |
| Overalls | **0.30** | Long-sleeve long gown (thick) | **0.46** |
| Coveralls | **0.49** | Long-sleeve short wrap robe (thick) | **0.48** |
| | | Long-sleeve pyjamas (thick) | **0.57** |
| | | Long-sleeve long wrap robe (thick) | **0.69** |



[2] © 2013, ASHRAE (www.ashrae.org). Used with permission from ASHRAE.

1 C. Henssge. Death time estimation in case work. I. The rectal temperature time of death Nomogram *Forensic Science International*, 38 (1988) 209 – 236.

2 J. Davey. Observations on the temperature of the human body after death. *Res. Physiol. Anat.* (London), 1 (1839) 228 – 248.

3 B. Hensley. Experiments on the temperature of bodies after death. *The Medical Examiner (Philadelphia*), 2 (March 1846) 149 – 152.

4 A. Taylor and D. Wilkes. On the cooling of the human body after death. *Guy's Hosp. Rep., (Oct. 1863)* 1809 – 211.

5 H. Rainy. On the cooling of dead bodies as indicating of time that has elapsed since death. *Glasg. Med. J.,* new series, 1:323 (1868 – 1869).

6 I. Newton. Scale gradum caliros. Calorium descriptiones & signa. *Philosophical Transactions of the Royal Society* (1701) London 824 – 829.

7 J.W. Burman. On the rate of Cooling of the human body after death. *Edin. Med. J.*, 25 (1880) 993.

8 F. Womack. The rate of body cooling after death, *St Barts Hosp. Rep.*, 23 (1887) 193.

9 F. Schwarz and H. Heidenwolf. Post mortem cooling and its relation to the time of death. *International Criminal Police Review*, 73 (1953) 339 – 344.

10 H. Shapiro. Medico-legal mythology: the time of death. *Journal of Forensic Medicine*, 1(3) (1954) 1 – 159.

11 H. Shapiro. The post-mortem plateau. *Journal of Forensic Medicine*, 12 (1965) 137 – 141.

12 G.S.W. de Saram, G. Webster and N. Kathirgamatamby. Post-mortem temperature and time of death. *The Journal of Criminal Law, Criminology and Police Science,* 46 (1955) 562 – 577.

13 H. Lyle and F. Cleaveland. Determination of the time since death by heat loss. *Journal of Forensic Science*, 1 (1956) 11 – 24.

14 G.S.W. de Saram, G. Webster. Estimation of death by medical criteria. *Journal of Forensic Medicine*, 4(2) (1957) 47.

15 F.S. Fiddes, T.D. Patten. A percentage method for representing the fall in body temperature after death. *Journal of Forensic Medicine*, 5 (1958) 2 – 15.

16 K. Sellier. Determination of the time since death by extrapolation of the temperature decrease curve. *Journal of Forensic Science*, 46(2) (1958) 317 – 322.

17 T. Marshall. The cooling of the body after death. MD Thesis, Leeds University, 1960.

18 T.K. Marshall. Estimating the time of death. *Journal of Forensic Science*, 7 (1962) 56 – 81.

19 T.K. Marshall. Estimating the time of death. *Journal of Forensic Science*, 7 (1962) 189 – 210.

20 T.K. Marshall. Estimating the time of death. *Journal of Forensic Science*, 7 (1962) 211 – 221.

21 T. K. Marshall. Temperature methods of estimating the time of death. *Medicine Science and Law*, 5 (1965) 224 – 232.

22 T.K. Marshall, F.E. Hoare. Estimating the time of death. The rectal cooling after death and its mathematical expression. *Journal of Forensic Science,* 7 (1962) 56 – 81.

23 T.K. Marshall. The use of the cooling formula in the study of the post mortem cooling. *Journal of Forensic Sciences*, 7 (1962) 189 – 210.

24 T.K. Marshall. The use of body temperature in estimating the time of death and its limitations. *Medicine, Science and Law*, 9 (1969) 178 – 182.

25 W.R.L. James, B.H. Knight. Errors in estimating time since death. *Med. Sci. Law.*, 5 (1965) 111 – 116.

26 A. Joseph and A. Schickele. A general method of assessing factors controlling post-mortem cooling. *American Academy of Forensic Sciences*, 15 (1970) 364 – 391.

27 A. Brown and T.K. Marshal. Body temperature as a means of estimating the time of death. *Forensic Science International*, 4 (1974) 125-133.

28 J. Simonsen, J. Voigt, N. Jeppesen, Determination of the time of death by continuous post-mortem temperature measurements, *Med. Sci. Law* 17 (1977) 112–122.

29 L.A. Kuehn, P. Tikuisis, S. Livingstone, R. Limmer. Body cooling after death. *Journal of Canadian Society of Forensic Science*, 12 (1979) 364 – 391.

30 L.A. Kuehn, P. Tikuisis, *et al*. Body cooling after death. *Aviat. Space Environ. Med.*, (Sept. 1980) 956 – 969.

31 K. Hiraiwa, Y. Ohno, F. Kuroda, I.M. Sebetan, S. Oshida. Estimation of the postmortem interval from rectal temperature by use of computer. *Medicine Science and Law*, 20 (2) (1980) 115 – 125.

32 K. Hiraiwa, T. Kudo, F. Kuroda, Y. Ohno, I.M. Sebetan, S. Oshida. Estimation of the post-mortem interval from rectal temperature by use of computer – Relationship between the rectal and skin cooling curves. *Medicine Science and Law*, 21(1) (1981) 4 – 9.

33 C. Henssge. Die Prazision von Todeszeitchatzungen durch die mathematische Beschriebung der rektalen Leichenbkuhlung (Precision of estimating the time of death by mathematical expression of rectal body cooling. German, summary in English) . *Zeit. Rechtsmed.,* 83 (1979) 45 – 67.

34 C. Henssge. Todeszeitchatzungen durch die mathematische beschriebung der rectalen Leichenabkuhlung unter verschienden Abkuhlungsbedingungen (Estimation of death-time by computing the rectal body cooling under various cooling conditions. German, summary in English). *Zeit. Rechtsmed.,* 87 (1981) 147 – 178.

35 C. Henssge, S. Hahn, B. Madea. Praktische Erfahrungen mit einem Abkühlungdummy. (Practical experience with a body-cooling dummy. German, summary in English). *Beitr. Gerichtl. Med.*, 44 (1986) 123 – 126.

36 C. Henssge , B. Madea, U. Schaar and C. Pitzken. Die Abkühlung eines Dummy unter verschiedenen Bedingungen im Vergleich zur Leichenabkühlung (The cooling of a dummy under various conditions in comparison with body cooling. German, summary in English). *Beitr Gerichtl Med* 45, (1987) 145–149.

37 L. Althaus, C. Henssge. Rectal temperature time of death nomogram: sudden change of ambient temperature. *Forensic Science International*, 99 (1999) 171 – 178.

38 P. Bisegna, C. Henβge, L. Althaus, G. Giusti. Estimation of the time since death: Sudden increase of ambient temperature. *Forensic Science International*, 176 (2008) 196 – 199.

39 A. Albrecht, I. Gerling, C. Henβge, M. Hochmeister, M. Kleiber, B. Madea, M. Oehmichen, St. Pollak, K. Püschel, D. Seifert, K. Teige. Zur Anwendung des Rektaltemperatur-Todsedzeit-Nomogramms am leichenfundort (Use of rectal temperature-time of death nomograms at the scene of death. German, Summary in English). *Z. Rechtsmed.* 103(4) (1990) 257 – 278.

40 C. Henssge. Rectal temperature time of death nomogram: Dependence of corrective factors on body weight under stronger thermic insulation conditions. *Forensic Science International*, 54:1 (1992) 51 – 66.

41 C. Henssge, B. Madea, E. Gallenkemper. Death time estimation in case work II. Integration of different methods. *Forensic Science International*, 39 (1988) 77 – 87.

42 C. Henssge, L. Altause, J. Bolt, A. Friesslederer, H. T. Haffner, C. A. Henssge, B. Hoppe, V. Schneider. Experiences with a compound method of estimating the time since death. II Intergration of non-temperature-based methods. *International Journal of Legal Medicine*, 113 (2000) 320 – 331.

43 C. Henssge, B. Madea, E. Gallenkemper. Todeszeitbestimmung – Integration verscheidener Teilmethoden (Estimation of time of death – Integration of different methods. German, Summary in English). *Zeitchtsmedizin für Rechtsmedizin,* 95 (1985) 185 – 196.

44 C. Henssge, B. Madea. Estimation of the time since death in the early post-mortem period. *Forensic Science International,* 144 (2004) 176 – 175.

45 L.M. Al-Alousi, R. A. Anderson. Microwave thermography in forensic medicine. *Police Surg.*, 30 (1986) 30 – 42.

46 L.M. Al-Alousi, R. A. Anderson, D. V. Land. A non-invasive method of temperature measurements using a microwave probe. *Forensic Science International*, 64 (1994) 35 – 46.

47 L.M. Al-Alousi, R. A. Anderson, D.M. Worster, D.V. Land. Multiple-probe thermography for estimating the post-mortem interval: I. Continuous monitoring and data analysis of brain, liver, rectal and environmental temperature in 117 forensic cases. *Journal of Forensic Science*, 46 (2) (2001) 317 – 322.

48 L.M. Al-Alousi, R. A. Anderson, D.M. Worster, D.V. Land. Multiple-probe thermography for estimating the post-mortem interval: II. Practical versions of the Triple-Exponential Formulae (TEF) for estimating the time of death in the field. *Journal of Forensic Science*, 46(2) (2001) 323 – 327.

49 L. M. Al-Alousi. A study of the shape of the post-mortem curve in 117 forensic cases. *Forensic Science International*, 125 (2002) 237 – 244.

50 L.M. Al-Alousi. R. A. Anderson, D.M. Worster, D.V. Land. Factors influencing the precision of estimating the post-mortem interval using the triple-exponential formulae (TEF) Part I: A study of the effect of body variables and covering of the torso on the postmortem brain, liver and rectal cooling rates in 117 forensic cases. *Forensic Science International*, 125 (2002) 223 – 230.

51 L.M. Al-Alousi. R. A. Anderson, D.M. Worster, D.V. Land. Factors influencing the precision of estimating the post-mortem interval using the triple-exponential formulae (TEF) Part II: A study of the effect of body temperature at the moment of death on the post-mortem brain, liver and rectal cooling in 117 forensic cases. *Forensic Science International*, 125 (2002) 231 – 236.

52 L.D.M. Nokes, A. Brown and B. Knight. A self-contained method for determining time since death from temperature measurements. *Medicine Science and Law*, 23 (1983) 166 – 170.

53 M.A. Green, J.C. Wright. Post-mortem interval estimation from body temperature data only. *Forensic Science International*, 28 (1985) 35 – 46.

54 M. A. Green, J. C. Wright. The theoretical aspects of the time dependent Z equation as a means of postmortem interval estimation using body temperature data only. *Forensic Science International*, 28 (1985) 53 – 61.

55 L. Nokes, B. Hicks, B. Knight. The post-mortem temperature plateau – fact or fiction? *Medicine Science and Law*, 25 (1985) 263 – 264.

56 E.L. Nelson Estimation of short-term postmortem interval utilizing core body temperature: a new algorithm. *Forensic Science International*, 109 (2000) 31- 38.

57 J.L. Smart and M. Kaliszan. The post-mortem temperature plateau and its role in the estimation of time of death. *Legal Medicine*, 14 (2012) 55 – 62.

58 G. Mall, W. Eisenmenger. Estimation of time since death by heat-flow Finite-element model part I: method, model, calibration and validation. *Legal Medicine* (2005) 1 – 14.

59 G. Mall, W. Eisenmenger. Estimation of time since death by heat-flow Finite-element model part II: application to non-standard cooling conditions and preliminary results in practical casework. *Legal Medicine*, 7 (2005) 69 – 80.

60 J.L. Smart. Estimation of the time of death with a Fourier series unsteady-state heat transfer model. *Journal of Forensic Science*, 55(6) (2010) 1481 – 1487.

61 L. Althaus, S. Stückradt, C. Henβge, T. Bajanowski. Cooling experiments using dummies covered by leaves. *International Journal of Legal Medicine,* 121 (2007) 112 – 114.

62 M. J. Eagle, P. Rooney, J. N. Kearney. Investigating the warming and cooling rates of cadavers by development of a gel-filled model to validate core temperature. *Cell Tissue Banking*, 8 (2007) 297 – 302.

63 J. Currie. Medical reports on the effects of water, cold and warm. London: Cadell & Davies, 1798; 20 – 25.

64 L. Alexander. The treatment of shock from prolonged exposure to cold, especially in water. Combined Intelligence Objective Subcommiettee. Item No. 24 File No. 1945; 26 – 37.

65 E.L. Lloyd. Accidental Hypothermia. *Resuscitation,* 32 (1996) 111 – 124.

66 A.S.T. Blake, G.W. Petley, C.D. Deakin. Effects of changes in packed cell volume on the specific heat capacity of blood: implications for studies measuring heat exchange in extracorporeal circuits. *British Journal of Anaesthesia*, 84 (2000) 28 – 32.

67 S. Smith, K. Simpson. Taylor's principles and practices of medical jurisprudence. 11th Ed. London 1956.

68 C. Henssge, B. Madea. Estimation of the time since death. *Forensic Science International*, 165 (2007) 182 – 184.

69 http://www.akts.com/thermal-safety-overview.html

70 J. Werner and M. Buse. Temperature profiles with respect to inhomogeneity and geometry of the human body. *Journal of Applied Physiology*, 65:3 (1988) 1110 – 1118.

71 J. Mead and C. L. Bonmarito. Reliability of rectal temperatures as an index of internal body temperature. *Journal of Applied Physiology,* 2 (1949) 97 – 109.

72 C. Newitt, M.A. Green. A Thermographic Study of Surface Cooling of Cadavers. *Journal of Forensic Science Society*, 19 (1979) 179 – 181.

73 G. Mall, M. Hubig, G. Beier, A. Büttner, W. Eisenmenger. Determination of time-dependent skin temperature decrease rates in the case of abrupt changes of environmental temperature. *Forensic Science International*, 113 (2000) 219 – 226.

74 http://www.engineeringtoolbox.com/thermal-conductivity-metals-d_858.html

75 http://people.bath.ac.uk/absmaw/BEnv1/properties.pdf

76 H.S. Carslow, J.C. Jaeger. Conduction of heat in solids. Clarendon Press,1959.

77 F.S. Fiddes, T.D. Patten. A percentage method for representing the fall in body temperature after death. *Journal of Forensic Medicine*, 5 (1958) 2 – 15.

78 Thermal Comfort chapter, Fundamentals volume of the ASHRAE Handbook, ASHRAE, Inc., Atlanta, GA, 2005.

79 M. Hubig, H. Muggenthaler, I. Sinicina, G. Mall. *International Journal of Legal Medicine*, 125(3)(2011) 437 – 444.

80 D.G. Smith. Numerical solution of partial differential equation. London, Oxford University Press (1965).

81 L. Lynnerup. A computer program for the estimation of time of death. *Journal of Forensic Sciences*, 38 (4) (1993) 816 – 820.